AC OPF in Radial Distribution Networks - Part I: On the Limits of the Branch Flow Convexification and the Alternating Direction Method of Multipliers

Konstantina Christakou, *Member, IEEE*, Dan-Cristian Tomozei, *Member, IEEE*, Jean-Yves Le Boudec, *Fellow, IEEE*, Mario Paolone, *Senior Member, IEEE*

***Abstract*—The optimal power-flow problem (OPF) has always played a key role in the planning and operation of power systems. Due to the non-linear nature of the AC power-flow equations, the OPF problem is known to be non-convex, therefore hard to solve. Most proposed methods for solving the OPF rely on approximations (e.g., of the network model) that render the problem convex, but that consequently yield inexact solutions. Recently, Farivar and Low proposed in [1,2] a method that is claimed to be exact for the case of radial distribution systems under specific assumptions, despite no apparent approximations. In our work, we show that it is, in fact, not exact. On one hand, there is a misinterpretation of the physical network model related to the ampacity constraint of the lines' current flows and, on the other hand, the proof of the exactness of the proposed relaxation requires unrealistic assumptions related to the unboundedness of specific control variables. Therefore, there is a need to develop algorithms for the solution of the non-appproximated OPF problem that remains inherently non-convex. Recently, several contributions have proposed OPF algorithms that rely on the use of the alternating-direction method of multipliers (ADMM). However, as we show in this work, there are cases for which the ADMM-based solution of the non-relaxed OPF problem fails to converge. To overcome the aforementioned limitations, we propose a specific algorithm for the solution of a non-approximated, non-convex OPF problem in radial distribution systems. In view of the complexity of the contribution, this work is divided in two parts. In this first part, we specifically discuss the limitations of both BFM and ADMM to solve the OPF problem.**

***Index Terms*—OPF, ADMM, decomposition methods, method of multipliers, convex relaxation, active distribution networks.**

I. INTRODUCTION

THE category of optimal power-flow problems (OPFs) represents the main set of problems for the optimal operation of power systems. The first formulation of an OPF problem appeared in the early 1960s and has been well-defined ever since [3]. It consists in determining the operating point of controllable resources in an electric network in order to satisfy a specific network objective subject to a wide range of constraints. Typical controllable resources considered in the literature are generators, storage systems, on-load tap changers (OLTC), flexible AC transmission systems (FACTS) and loads (e.g., [4]–[8]). The network objective is usually the minimization of losses or generation costs, and typical constraints include power-flow equations, capability curves of the controllable resources, as well as operational limits on the line power-flows and node voltages (e.g., [9]).

The OPF problem is known to be non-convex, thus difficult to solve efficiently (e.g., [10]–[12]). Since the problem was first formulated, several techniques have been used for its solution. Among others, non-linear and quadratic programming techniques, Newton-based methods, interior point methods in the earlier years, as well as heuristic approaches based on genetic algorithms, evolutionary programming, and particle-swarm optimization in recent years (e.g., [13]–[15]).

Currently, the OPF problem is becoming more compelling due to the increasing penetration of embedded generation in distribution networks, essentially composed by renewable resources. The distributed nature of such resources, as well as their large number and potential stochasticity increase significantly the complexity of the OPF problem and bring about the need for distributed solutions. In this direction, several distributed algorithms have been proposed in the literature. In [16,17] the authors design a dual-ascent algorithm for optimal reactive power-flow with power and voltage constraints. In [18,19] dual decomposition is used as the basis for the distributed solution of the OPF problem. Finally, a significant number of contributions propose distributed formulations of the OPF problem that are based on the alternating direction method of multipliers (ADMM) (e.g., [18,20]–[24]).

However, due to the non-convex nature of the problem, most of the proposed schemes either do not guarantee to yield an optimal solution or they are based on approximations that convexify the problem in order to guarantee convergence. These approximations, often, either lead to (i) misinterpretation of the system model [25] or (ii) solutions that, even though mathematically sound, might be far away from the real optimal solution, thus having little meaning for the grid operation [26].

Recently, Farivar and Low proposed in [1,2] a convexification of the problem that is claimed to be exact for radial networks. In Part I of this paper, we show that this claim is not exact, as the convexification of the problem leads to an inexact system model. We also show that the method of ADMM-based decomposition, which comes together with the convexification, does not work for a correct system model. As an alternative, we propose in Part II an algorithm for the solution of the correct AC OPF problem in radial networks. Like ADMM, it uses an augmented Lagrangian, but unlike ADMM, it uses primal decomposition [27] and does not require that the problem be convex. We consider a direct-

Konstantina Christakou, Dan-Cristian Tomozei, Jean-Yves Le Boudec and Mario Paolone (email: konstantina.christakou@epfl.ch, dan-cristian.tomozei @epfl.ch, jean-yves.leboudec@epfl.ch, mario.paolone@epfl.ch) are with the École Polytechnique Fédérale de Lausanne, CH-1015 Lausanne, Switzerland.

sequence representation of the electric distribution grid and we present both a centralized and a decentralized asynchronous version of the algorithm.

The structure of this first part is as follows. In Section II we present the generic formulation of the OPF problem in radial distribution systems and we classify several OPF algorithms based on the approximations and assumptions on which they rely. In Section III we discuss the limitations and applicability of the Farivar-Low formulation of the OPF problem proposed in [1,2]. We provide, in Section IV, the ADMM-based solution of the original non-approximated OPF problem. In the same section, we highlight specific cases where the ADMM-based algorithm fails to converge. Finally, we provide the main observations and concluding remarks for this part in Section V.

II. Generic Formulation Of The OPF Problem

In the rest of the paper, we consider a balanced radial network composed of buses ($\mathcal{B}$), lines ($\mathcal{L}$), generators ($\mathcal{G}$) and loads ($\mathcal{C}$). The network admittance matrix is denoted by Y. Several generators/loads can be connected to a bus $b\in\mathcal{B}$. We denote that a generator $g\in\mathcal{G}$ or a load $c\in\mathcal{C}$ is connected to a bus by "$g\in b$" and "$c\in b$". A line $\ell\in\mathcal{L}$ is represented using a π-equivalent model and it has a receiving and a sending end denoted by ℓ^+ and ℓ^-. Each line is connected to two adjacent buses: $\beta(\ell^+)$ and $\beta(\ell^-)$, respectively.

A. Generic OPF Formulation

The traditional formulation of the OPF problem consists in minimizing a specific network objective:

$$\min_{\bar{S}_g,\bar{S}_c,\bar{S}_\ell^+,\bar{S}_\ell^-,\bar{I}_\ell^+,\bar{I}_\ell^-,\bar{V}_b} \sum_{g\in\mathcal{G}} C_g(\bar{S}_g) + \sum_{c\in\mathcal{C}} C_c(\bar{S}_c) \tag{1}$$

The first term of the network objective (C_g) in (1) is typically a non-decreasing convex function accounting for the minimization of the generation costs or the network real power losses. The second term (C_c) is included in the objective when the cost of non-supplied load is taken into account.

The following set of constraints is considered[1]:

$$\sum_{g\in b}\bar{S}_g - \sum_{c\in b}\bar{S}_c + \sum_{\beta(\ell^+)=b}\bar{S}_{\ell^+} + \sum_{\beta(\ell^-)=b}\bar{S}_{\ell^-} = 0, \quad \forall b\in\mathcal{B} \tag{2}$$

$$\bar{S}_{\ell^+} = \bar{V}_{\beta(\ell^+)}\underline{I}_{\ell^+}, \quad \bar{S}_{\ell^-} = \bar{V}_{\beta(\ell^-)}\underline{I}_{\ell^-}, \quad \forall\ell\in\mathcal{L} \tag{3}$$

$$\bar{I}_{\ell^+} = \bar{Y}_\ell(\bar{V}_{\beta(\ell^+)} - \bar{V}_{\beta(\ell^-)}) + \bar{Y}_{\ell_0^+}\bar{V}_{\beta(\ell^+)}, \quad \forall\ell\in\mathcal{L} \tag{4}$$

$$\bar{I}_{\ell^-} = \bar{Y}_\ell(\bar{V}_{\beta(\ell^-)} - \bar{V}_{\beta(\ell^+)}) + \bar{Y}_{\ell_0^-}\bar{V}_{\beta(\ell^-)}, \quad \forall\ell\in\mathcal{L} \tag{5}$$

$$V_{min} \leq |\bar{V}_b| \leq V_{max}, \quad \forall b\in\mathcal{B} \tag{6}$$

$$|\bar{S}_{\ell^+}| \leq S_{\ell_{max}}, \quad \text{or} \quad |\bar{I}_{\ell^+}| \leq I_{\ell_{max}}, \quad \forall\ell\in\mathcal{L} \tag{7}$$

$$|\bar{S}_{\ell^-}| \leq S_{\ell_{max}}, \quad \text{or} \quad |\bar{I}_{\ell^-}| \leq I_{\ell_{max}}, \quad \forall\ell\in\mathcal{L} \tag{8}$$

$$\bar{S}_g \in \mathcal{H}_g, \quad \forall g\in\mathcal{G} \quad \text{and} \quad \bar{S}_c\in\mathcal{H}_c, \quad \forall c\in\mathcal{C} \tag{9}$$

where, $\bar{S}$ denotes the complex power[2], $\bar{V}_b$ is the direct sequence phase-to-ground voltage of node b, $\bar{I}_{\ell^+}$ ($\bar{I}_{\ell^-}$) is the current flow in the receiving (sending) end of line ℓ, $\bar{Y}_\ell$ is the longitudinal admittance of a line, $\bar{Y}_{\ell_0^+}$ ($\bar{Y}_{\ell_0^-}$) is the shunt capacitance at the receiving (sending) end of the line, and $\mathcal{H}_g, \mathcal{H}_c$ are the capability curve of the generator g and the limits of the load c respectively[3]. If a generator (load) is non-controllable then the set $\mathcal{H}_g$ ($\mathcal{H}_c$) is limited to a single point.

The first constraint (2) corresponds to the power balance constraint at each network bus, whereas (3) is an alternative way to define the AC power flow equations. Constraints (6) and (7) are so-called node voltage and lines ampacity contraints, i.e., limits on node voltages and line power/current flows. The last constraints (9) represent the capability limits that each of the controllable devices should respect.

The equality constraints (3) render the OPF problem non-convex and, therefore, difficult to solve efficiently. The majority of the proposed algorithms in the literature rely on several approximations and/or convex relaxations and seek a solution to a modified OPF problem. In what follows, we describe and discuss the most common approximations.

B. Approximations of the OPF problem

In general, the approximations used in the formulation of an OPF problem can be categorized in two large groups: approximations of the physical network models and methods that relax the space of the solutions and/or control variables.

In the first case, we can find OPF formulations that rely mainly on linearizations of the AC power flow equations. Such attempts typically (i) consider the DC power flow, (ii) use the decoupled AC power flow or (iii) neglect the network losses and/or the transverse parameters of the lines. Specifically, the concepts of the DC and the decoupled OPF have been extensively used in the literature (e.g., [28]–[31]), as they approximate the OPF problem with linear programming problems and, therefore, enable its fast resolution. Furthermore, the authors in [22] use the so-called Dist-Flow equations ([32]) to linearize the power flows and propose an ADMM-based OPF algorithm that neglects the real and reactive losses. Finally, several contributions rely on simplified network line-models that neglect the transverse parameters, resulting in inaccuracies of the physical system model (e.g., [33]–[35]).

In the second case, we can find OPF formulations where, typically, the constraints are relaxed in order to convexify the problem. In particular, a large number of contributions recently proposed a SDP formulation of the OPF problem, where the rank-one constraint of a matrix is relaxed and the algorithm is claimed to yield zero-duality gap for radial distribution networks (e.g., [18,19,36]). Another relaxation is proposed in [35] where the OPF problem is cast as a second order cone programming. A similar technique is used in [37], where the equality constraints of the branch flows are relaxed.

In both the aforementioned categories of approximations, the modified OPF formulations guarantee convergence of the proposed algorithms. The reached solutions, however, even though mathematically sound, are not always meaningful for the grid operation. The DC and the decoupled OPF work sufficiently well for transmission systems, nevertheless they can introduce large errors when used for solving the OPF

[1]In the rest of the paper, complex numbers are denoted with a bar above (e.g., $\bar{V}$) and complex conjugates with a bar below (e.g.,$\underline{V}$).

[2]We use the convention that positive values represent power injection and negative power consumption.

[3]Note that different types of controllable generators or loads can be accounted for via their corresponding capability curves/limits.

in the case of distribution systems (e.g., [38]). As far as the semidefinite relaxation is concerned, its limitations have been recently investigated. The authors in [26] show through practical examples, that in the case of negative locational marginal prices or strict line-flow constraints it can lead to solutions that are not valid, namely for which the duality gap is not zero. Furthermore, in [39] the authors show the existence of multiple local optima of the OPF problem due to the feasible region being disconnected and due to the nonlinearities of the constraints; they show that the SDP formulation of the OPF problem fails to find the global optimum in cases where there are multiple local optima. In the same direction, a recent review ([34]) summarizes the semidefinite relaxations applied to the OPF problem and discusses their limitations.

Recently, another formulation of the OPF problem has been proposed ([1,2,40]–[42]). This formulation also belongs to the category of the semidefinite relaxations and uses the so-called branch-flow model (BFM) for describing the network. The BFM essentially describes the network flows by using as variables the currents and the powers of the various network branches, instead of the nodal injections. In [1,2] Farivar and Low propose an OPF formulation that relies on the BFM representation of the network and they present a two-step relaxation procedure that turns the problem into a second-order cone program (SOCP). The authors prove that under specific assumptions both relaxation steps are exact for the case of radial networks, hence a globally optimal OPF solution can be retrieved by solving the relaxed convex problem.

In what follows, we first briefly recall the Farivar-Low formulation of the OPF problem and then we investigate the applicability of the branch flow model to the OPF formulation. We show, on one hand, that the Farivar-Low model misinterprets the physical network model by imposing an ampacity constraint on a fictitious line-current flow that neglects the contribution of the shunt components of the line and that, on the other hand, the proof of the exactness of the proposed relaxation requires unrealistic assumptions related to the unboundedness of specific control variables.

III. On the Limits of the Farivar-Low approach for the Solution of the OPF Problem

A. The Farivar-Low Formulation of the OPF problem

We assume the same objective function as in Eq. 1 and again consider that the network lines are represented using a π-model. Contrary to the formulation in (2)-(9), we reformulate the constraints of the OPF problem by using the branch power and current flows as variables, similarly to [1]. To this end, we denote by $\bar{S}_\ell$ and $\bar{I}_\ell$ the power and the current that flow across the longitudinal elements of a network line ℓ from the receiving toward the sending end, for which it holds that

$$\bar{I}_\ell = \bar{Y}_\ell(\bar{V}_{\beta(\ell^+)} - \bar{V}_{\beta(\ell^-)}), \quad \forall \ell \in \mathcal{L} \tag{10}$$

$$\bar{S}_\ell = \bar{V}_{\beta(\ell^+)} \underline{I}_\ell, \quad \forall \ell \in \mathcal{L} \tag{11}$$

The power and current flows along the shunt elements of the lines are taken into account in the bus power balance constraints as nodal injections. In this direction, we denote by $\bar{Y}_{b_0}$ the sum of all the shunt elements of the lines that are adjacent to bus b. Hence, the constraints of the OPF problem are reformulated as follows by Farivar and Low:

$$\sum_{g \in b} \bar{S}_g - \sum_{c \in b} \bar{S}_c = \sum_{\beta(\ell^+)=b} \bar{S}_\ell - \sum_{\beta(\ell^-)=b} (\bar{S}_\ell - \bar{Y}_\ell^{-1}|\bar{I}_\ell|^2) - \bar{Y}_{b_0}|\bar{V}_b|^2, \; \forall b \in \mathcal{B} \tag{12}$$

$$|\bar{I}_\ell|^2 = \frac{|\bar{S}_\ell|^2}{|\bar{V}_{\beta(\ell+)}|^2}, \; \forall \ell \in \mathcal{L} \tag{13}$$

$$|\bar{V}_{\beta(\ell-)}|^2 = |\bar{V}_{\beta(\ell+)}|^2 + |\bar{Y}_\ell^{-1}|^2 |\bar{I}_\ell|^2 - (\bar{Y}_\ell^{-1} \underline{S}_\ell + \underline{Y}_\ell^{-1} \bar{S}_\ell), \; \forall \ell \in \mathcal{L} \tag{14}$$

$$V_{min}^2 \leq |\bar{V}_b|^2 \leq V_{max}^2, \; \forall b \in \mathcal{B} \tag{15}$$

$$|\bar{I}_\ell|^2 \leq I_{\ell_{max}}^2, \; \forall \ell \in \mathcal{L} \tag{16}$$

$$Re(\bar{S}_g) \in [P_{g_{min}}, P_{g_{max}}], Im(\bar{S}_g) \in [Q_{g_{min}}, Q_{g_{max}}], \; \forall g \in \mathcal{G} \tag{17}$$

$$Re(\bar{S}_c) \in [P_{c_{min}}, P_{c_{max}}], Im(\bar{S}_c) \in [Q_{c_{min}}, Q_{c_{max}}], \; \forall c \in \mathcal{C} \tag{18}$$

Note that in the Farivar-Low formulation of the OPF problem, the capability curves of the controllable loads and generators, i.e., constraints (17,18) on the nodal power $\bar{S}$ are limited to rectangular regions. This is essential for the conic relaxation proposed in [1,2].

Starting from this formulation, Farivar and Low relax the equality constraints in (13) to inequalities and cast the aforementioned problem as a second-order cone program. They also prove that for radial networks a global solution of the original OPF problem can be recovered from the solution of the relaxed problem if there are no upper bounds on the loads. In other words, Farivar and Low solve (12)-(18) by setting $P_{c_{max}}$=∞ and $Q_{c_{max}}$=∞ in constraint (18).

We show, in what follows, that this formulation is not equivalent to (1-9). In particular, constraint (16) (constraint (9) in [1]) is only an approximation of the ampacity constraints and, moreover, the assumptions on the controllability and bounds of the energy resources in the network are unrealistic.

B. Misinterpretation of the Physical Network Model in the Farivar-Low OPF Formulation

The branch-flow model has been often used in load-flow studies (e.g., [43,44]) and constitutes an accurate representation of the network model. The first problem with the Farivar-Low formulation in (12)-(18) is that it misinterprets the physical network model when constraining the line flows in the network. Even though the power-flow equations in (12)-(14) are exact when the shunt capacitances are considered as nodal injections, the constraint (16) is imposed on a fictitious current flow across the longitudinal component of the lines, thus *does not* account for the current flow toward the shunt elements. Therefore, the optimum of problem (12)-(18) can be such that the line ampacity constraint is violated.

To better clarify why this occurs, we use a single-branch toy network, as shown in Fig. 1. The line parameters, as well as the base values of the system are given in Table I. A purely resistive load is connected to bus 2 that we vary linearly in the range of $[100 - 10000]$Ohms in order to numerically quantify the mismatch between those quantities. We measure the current flows at the two ends of the line, as well as the flow along the longitudinal impedance of the line. Fig. 2 shows the measured quantities as a function of the load. It can be observed that the current flowing across the longitudinal impedance of the line under-estimates the actual current flow in the receiving end of the line.

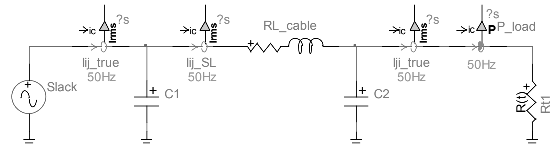

Fig. 1. The test network used for the numerical comparison of the current flows at the sending/receiving end of the lines and the current flow along the longitudinal line impedance.

Table I
PARAMETERS OF THE TEST NETWORK IN FIG.1

Parameter	Value
Network rated voltage, V(kV)	15
Line parameters, R(Ohms), L(H), C(uF)	(1,0.003,0.54)

As a consequence, in the Farivar-Low formulation setting the limit on the longitudinal current flow below the line ampacity does not guarantee that the actual line current will respect this limit. In order to illustrate such a scenario, we consider yet another simple test network shown in Fig. 3. All the network lines are built by using the same values of resistance, reactance and capacitance per km, but by assuming different values of their length[4]. We assume a first test case where the controllable device connected to bus 4 is a generator, whereas controllable loads are connected to buses 2 and 3. The network characteristics, the base values, the capability limits of the controllable resources[5], and the voltage and ampacity bounds are provided in Table II. We assume that the controllable generation operates at a unity power factor. The problem in (12)-(18) is formulated and solved in Matlab. The objective function accounts for loss minimization, as well as utility maximization of the controllable generation units:

$$\min_{\bar{S}_g, \bar{S}_\ell, |\bar{V}_b|, |\bar{I}_\ell|} -\sum_{g\in\mathcal{G}} Re(\bar{S}_g) + \sum_{\ell\in\mathcal{L}} Re(\bar{Y}_\ell)|\bar{I}_\ell|^2 \qquad (19)$$

In order to investigate the order of magnitude of the violation of the ampacity constraint, we solve the OPF problem for various line lengths and network voltage-rated values. In particular, we assume that the line lengths are uniformly multiplied by a factor in the range $[1.25-7.5]$ (while keeping the network voltage rated value to its nominal value) and the network voltage rated value varies in the range $[15-45]kV$ (while keeping the line lengths to their nominal values). Once the optimal solution is computed in each case, we calculate

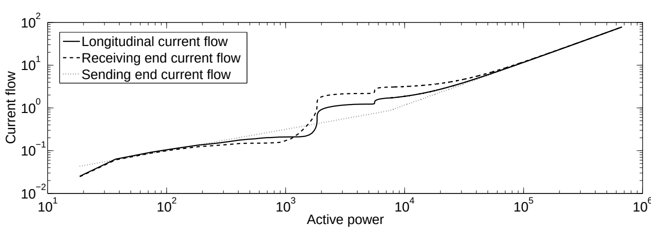

Fig. 2. Current flows at the sending/receiving end of the line and along the longitudinal line impedance (log-log scale).

[4]Typical values of medium-voltage underground cables are considered for the resistance, reactance and shunt capacitances of the lines.

[5]The upper bounds of the active and reactive power of the loads are considered to be infinite, as required in the Farivar-Low formulation.

Table II
PARAMETERS OF THE TEST NETWORK IN FIG.3 USED FOR THE INVESTIGATION OF THE LINE AMPACITY LIMIT VIOLATION

Parameter	Value
Network rated voltage and base power, V(kV),S(MVA)	24.9,5
Line parameters, R(Ohms/km), L(mH/km), C(uF/km)	(0.193,0.38,0.24)
$[P_{g_{min}}, P_{g_{max}}]$ (MW)	$[0, 2]$
$P_{c_{min}}$(MW) (bus2, bus3)	$(0.05, 0.06)$
$Q_{c_{min}}$(Mvar) (bus2, bus3)	$(0.03, 0.027)$
$[V_{min}, V_{max}]$ (p.u)	$[0.9, 1.1]$
I_{max} (A)	80

Table III
PARAMETERS OF THE TEST NETWORK IN FIG.3 USED FOR THE INVESTIGATION OF THE NETWORK OPERATING POINT ON THE LINE AMPACITY LIMIT VIOLATION

Parameter	Value
$[P_{g_{min}}, P_{g_{max}}]$(MW) (bus 2)	$[0, 0.01]$
$[P_{g_{min}}, P_{g_{max}}]$(MW) (bus 3)	$[0, 0.012]$
$(P_{c_{min}}, Q_{c_{min}})$(MW,Mvar) (bus 4)	$0.3, 0.15$

the actual current flows in the sending/receiving end of the lines and we compute the maximum constraint violation. The results are shown in Fig. 4. As the line length increases, the current flowing toward the shunt capacitors increases, thus neglecting its contribution to the line flow leads to significant violations of the ampacity limit. At 7.5 times the initial line length, the violation reaches a value of 18.4%. The effect of the network voltage-rated value is similar, with a maximum constraint violation of 25% when the voltage value is 45kV.

In addition to the effect of the line lengths and the network voltage-rated value, we study the effect of the network operating point on the ampacity violation. To this end, we consider a second test case where the controllable device connected to bus 4 is a load and generators are connected to buses 2 and 3. The capability limits of the controllable resources are provided in Table III. For this setting, Fig. 5 shows the solution of the Farivar-Low OPF problem, namely current flows at the receiving/sending end of the network lines, as well as across the longitudinal impedance. We can observe that the maximum violation of the ampacity constraint is in the order of 39.6%.

In order to avoid current flows that exceed the lines' ampacity limits, i.e., in order to use the BFM in an accurate

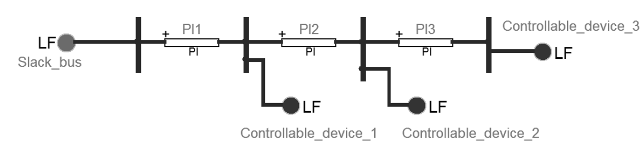

Fig. 3. Network used in the study of the Farivar-Low OPF formulation.

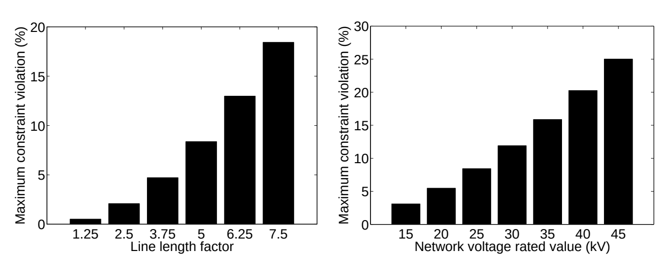

Fig. 4. Maximum ampacity constraint violation as a function of the line lengths and the network voltage rated value.

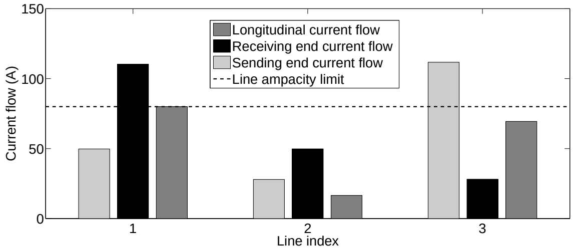

Fig. 5. Farivar-Low OPF solution for the current flows at the sending/receiving end of the network lines and across the longitudinal line impedance under heavy consumption and light generation conditions.

way, the Farivar-Low formulation should either consider the actual current flows in the receiving/sending ends of the lines as optimization variables, or should add the contribution of the current flows toward the shunt elements of the lines to the longitudinal current flow in the inequality constraint (16). By adopting either of the two approaches, however, (12)-(18) can no longer be solved efficiently as proposed in [1,2]. Therefore, the generic OPF problem cannot be convexified by using Farivar-Low's approach.

C. On the Assumptions Required for the Exactness of the Farivar-Low Relaxation

In addition to the aforementioned fundamental problem, which is related to the physical network model, Farivar and Low require specific assumptions to hold in order to prove the exactness of the proposed relaxations. Several of these assumptions are too strong and not realistic.

To begin with, the OPF formulation in [1,2] assumes controllability of both loads and generators in the network buses and, in particular, assumes rectangular bounds on the powers of loads/generators. This is quite a strong assumption, as usually the DNO has very few specific control points available in the network with capability curves that are typically more complex and that account, among others, for capabilities of power electronics and limitations of machinery. An even more serious limitation is that the Farivar-Low model considers no upper bounds on the controllable loads in order to prove the exactness of the proposed relaxation. This implies that in cases where excessive production of the generators causes violations of the voltage or line-flows limits, local demand is invoked to compensate for the increased generation. In order to illustrate such a setting and to show that the result of the OPF problem can result in unrealistic values for demand, we consider the same network in Fig. 3 and we assume that there is high penetration of distributed generation and a low demand. The values of loads and generation, as well as the corresponding limits are shown in Table IV. Solving the optimization problem and considering infinite upper bounds on the demand results in load values that are significantly increased, compared to the minimum values shown in Table IV. The resulting optimal power points are shown in Fig. 6. We show in black the initial values for active and reactive power of loads and generation (corresponding to the values of Table IV), and in gray the results of the OPF solution (when not accounting for upper

Table IV
PARAMETERS OF THE TEST NETWORK IN FIG.3 USED FOR THE INVESTIGATION OF THE UNBOUNDEDNESS OF THE CONSUMPTION

Parameter	Value
$[P_{g_{min}}, P_{g_{max}}]$ (MW)	$[0, 1.2]$
$(P_{c_{min}}, Q_{c_{min}})$ (MW,Mvar) (buses 2,3)	$(0.0125, 0.0026)$

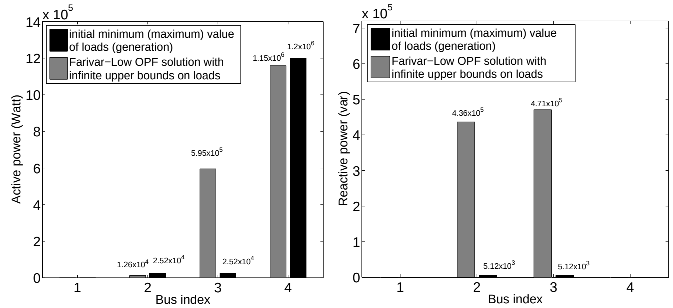

Fig. 6. Optimal solution of the Farivar-Low OPF formulation for the active and reactive power set-points when upper bounds on loads are infinite.

bounds on loads). It is worth observing that the optimal active power consumption of bus 3 is increased 23.6 times and the reactive power consumption at buses 2 and 3 is increased 85.3 and 92 times, respectively. In a realistic setting, even if part of the demand in the network is controllable, the amount of available demand-response is limited and such an increase in the consumption is most likely not possible. Therefore, in such a case, the congestion and voltage problems should be solved by properly controlling the generator within its capability limits. In addition to this, typically, the active and reactive power consumption should be linked via the corresponding power factor. We observe, however, that the OPF solution in this scenario results in very large values for the reactive power consumption and, in particular, the power factor of Bus 2 is 0.03 after the OPF solution, whereas initially its value is 0.98. In an attempt to relax this assumption, Farivar and Low claim that the infinite upper bound on the loads, when not applicable, can be replaced by equivalent conditions [42]. However, not only are these conditions unrealistic, they are also not applicable in our context as they require no upper bound on the voltage magnitudes. This is in contradiction with the actual problem we target, i.e., voltage rise due to high penetration of renewable energy resources.

Overall, the fundamental problems with the Farivar-Low approach, as well as with the several additional assumptions, prohibit its application to the generic OPF problem. As a consequence, there is a need to design algorithms that target the original non-approximated OPF problem that remains inherently non-convex. Recent trends are in favor of using ADMM for the solution of the OPF problem. Even though ADMM requires the underlying problem to be convex in order to guarantee convergence, it has been applied also to the case of non-convex AC OPF problems with promising convergence performance (e.g., [21,24]). In what follows we first present the ADMM solution of the problem in (1)-(9) and then we highlight specific scenarios for which ADMM fails to converge when applied to the non-approximated OPF problem.

IV. On the Application of ADMM for the Solution of the OPF Problem

A. ADMM-based Solution of the OPF Problem

The ADMM-based solution of the OPF problem requires that the control variables are split into two separate groups and that the objective function is separable across this splitting [45]. To this end, we introduce additional slack variables, $\bar{z}$, for the devices' and loads' power injections and for the line power flows and we reformulate the OPF problem as follows[6]:

$$\min_{\substack{\bar{S}_g,\bar{z}_g,\bar{S}_c,\bar{z}_c,\bar{S}_{\ell+},\bar{z}_{\ell+},\bar{S}_{\ell-}\\ \bar{z}_{\ell-},\bar{E}_{\ell+},\bar{E}_{\ell-},\bar{I}_{\ell+},\bar{I}_{\ell-}\bar{V}_b}} -\sum_g U_g(Re(\bar{S}_g)) + \sum_b J_V(|\bar{V}_b|) + \tag{20}$$
$$\sum_\ell J_I(|\bar{I}_\ell^+|,|\bar{I}_\ell^-|) + \sum_b \phi(\sum_{g\in b}\bar{z}_g - \sum_{c\in b}\bar{z}_c + \sum_{\beta(\ell^+)=b}\bar{z}_{\ell+} + \sum_{\beta(\ell^-)=b}\bar{z}_{\ell-})$$

$$\text{subject to: } \bar{S}_g = \bar{z}_g\,,\forall\, g\in\mathcal{G}, \quad \text{and} \quad \bar{S}_c = \bar{z}_c\,,\forall\, c\in\mathcal{C} \tag{21}$$
$$\bar{S}_{\ell+} = \bar{z}_{\ell+}, \quad \text{and} \quad \bar{S}_{\ell-} = \bar{z}_{\ell-}\,,\forall\,\ell\in\mathcal{L} \tag{22}$$
$$\bar{E}_{\ell+} = \bar{V}_{\beta(\ell^+)}, \quad \text{and} \quad \bar{E}_{\ell-} = \bar{V}_{\beta(\ell^-)}\,,\forall\,\ell\in\mathcal{L} \tag{23}$$

where ϕ is the characteristic function of the set $\{\bar{x}\in\mathbb{C} : \bar{x} = 0\}$, J_V is a penalty function with value 0 if $V_{min} \le |\bar{V}_b| \le V_{max}$ and ∞ otherwise and J_I is a penalty function with value 0 if $\max(|\bar{I}_\ell^+|,|\bar{I}_\ell^-|) \le I_{\ell_{max}}$ and ∞ otherwise.

The augmented Lagrangian for this problem is as follows:

$$L_\omega(\bar{S}_g,\bar{S}_c,\bar{S}_{\ell+},\bar{S}_{\ell-},\bar{E}_{\ell+},\bar{E}_{\ell-},\bar{I}_{\ell+},\bar{I}_{\ell-},\bar{z}_g,\bar{z}_c,\bar{z}_{\ell+},\bar{z}_{\ell-},\bar{V}_b,\bar{\mu},\bar{\nu},\bar{\lambda})$$
$$= -\sum_g U_g(Re(\bar{S}_g)) + \sum_b J_V(|\bar{V}_b|) + \sum_\ell J_I(|\bar{I}_\ell^+|,|\bar{I}_\ell^-|)$$
$$+\sum_b \phi(\sum_{g\in b}\bar{z}_g - \sum_{c\in b}\bar{z}_c + \sum_{\beta(\ell^+)=b}\bar{z}_{\ell+}\sum_{\beta(\ell^-)=b}\bar{z}_{\ell-})$$
$$+\frac{\omega}{2}\{\sum_\ell|\bar{E}_{\ell+} - \bar{V}_{\beta(\ell^+)} + \bar{\mu}_\ell|^2 + \sum_\ell|\bar{E}_{\ell-} - \bar{V}_{\beta(\ell^-)} + \bar{\nu}_\ell|^2$$
$$+\sum_g|\bar{S}_g - \bar{z}_g + \bar{\lambda}_g|^2 + \sum_c|\bar{S}_c - \bar{z}_c + \bar{\lambda}_c|^2$$
$$+\sum_\ell|\bar{S}_{\ell+} - \bar{z}_{\ell+} + \bar{\lambda}_{\ell+}|^2 + \sum_\ell|\bar{S}_{\ell+} - \bar{z}_{\ell-} + \bar{\lambda}_{\ell-}|^2\} \tag{24}$$

where $\bar{\mu},\bar{\nu},\bar{\lambda}$ are the lagrange multipliers associated with the equality constraints (21)-(23).

The ADMM algorithm at the $k-th$ iteration consists of the following steps:

1) First, all the devices, loads and lines update in parallel the primary variables, and their internal variables, i.e., $(\bar{S}_g,\bar{S}_c,\bar{S}_{\ell+},\bar{S}_{\ell-},\bar{E}_{\ell+},\bar{E}_{\ell-},\bar{I}_{\ell+},\bar{I}_{\ell-})$ with the secondary variables, and the dual variables fixed [7]:

For each network line ℓ:

$$(\bar{S}_{\ell+}^{k+1},\bar{S}_{\ell-}^{k+1},\bar{E}_{\ell+}^{k+1},\bar{E}_{\ell-}^{k+1},\bar{I}_{\ell+}^{k+1},\bar{I}_{\ell-}^{k+1}) =$$
$$\operatorname*{argmin}_{\bar{S}_{\ell+},\bar{S}_{\ell-},\bar{E}_{\ell+},\bar{E}_{\ell-},\bar{I}_{\ell+},\bar{I}_{\ell-}} J_I(|\bar{I}_\ell^+|,|\bar{I}_\ell^-|) +$$
$$\frac{\omega}{2}(|\bar{E}_{\ell+} - \bar{V}_{\beta(\ell^+)}^k + \bar{\mu}_\ell^k|^2 + |\bar{E}_{\ell-} - \bar{V}_{\beta(\ell^-)}^k + \bar{\nu}_\ell^k|^2$$
$$+|\bar{S}_{\ell+} - \bar{z}_{\ell+}^k + \bar{\lambda}_{\ell+}^k|^2 + |\bar{S}_{\ell-} - \bar{z}_{\ell-}^k + \bar{\lambda}_{\ell-}^k|^2) \tag{25}$$

$$\text{subject to: } \bar{S}_{\ell+} = \bar{E}_{\ell+}\underline{I}_{\ell+} \quad \text{and} \quad \bar{S}_{\ell-} = \bar{E}_{\ell-}\underline{I}_{\ell-} \tag{26}$$
$$\bar{I}_{\ell+} = \bar{Y}_\ell(\bar{E}_{\ell+} - \bar{E}_{\ell-}) + \bar{Y}_{\ell_0^+}\bar{E}_{\ell+} \tag{27}$$
$$\bar{I}_{\ell-} = \bar{Y}_\ell(\bar{E}_{\ell-} - \bar{E}_{\ell+}) + \bar{Y}_{\ell_0^-}\bar{E}_{\ell-} \tag{28}$$

For each device g: (29)

$$\bar{S}_g^{k+1} = \operatorname*{argmin}_{\bar{S}_g} -U_g(Re(\bar{S}_g)) + \frac{\omega}{2}(|\bar{S}_g - \bar{z}_g^k + \bar{\lambda}_g^k|^2)$$

subject to: $\bar{S}_g \in \mathcal{H}_g$

For each load c: $\bar{S}_c^{k+1} = \bar{S}_c$ (30)

2) Then, by using the updated primary variables, the secondary variables are updated, i.e.,$(\bar{z},\bar{V}_b)$, on a bus level. We denote by $\bar{z}_b$ the vector of complex powers of all the devices, loads and lines that are connected to bus b, i.e., $\bar{z}_b \triangleq (\bar{z}_{g:g\in b},\bar{z}_{c:c\in b},\bar{z}_{\ell^+:\beta(\ell^+)=b},\bar{z}_{\ell^-:\beta(\ell^-)=b})$:

$$\bar{z}_b^{k+1} = \operatorname*{argmin}_{\bar{z}_b}(\phi(\sum_{g\in b}\bar{z}_g - \sum_{c\in b}\bar{z}_c + \sum_{\beta(\ell^+)=b}\bar{z}_{\ell+}\sum_{\beta(\ell^-)=b}\bar{z}_{\ell-}) \tag{31}$$
$$+\frac{\omega}{2}\{\sum_{g\in b}|\bar{S}_g^{k+1} - \bar{z}_g + \bar{\lambda}_g^k|^2 + \sum_{c\in b}|\bar{S}_c^{k+1} - \bar{z}_c + \bar{\lambda}_c^k|^2$$
$$+\sum_{\beta(\ell^+)=b}|\bar{S}_{\ell+}^{k+1} - \bar{z}_{\ell+} + \bar{\lambda}_{\ell+}^k|^2 + \sum_{\beta(\ell^-)=b}|\bar{S}_{\ell-}^{k+1} - \bar{z}_{\ell-} + \bar{\lambda}_{\ell-}^k|^2\})$$

$$\bar{V}_b^{k+1} = \operatorname*{argmin}_{\bar{V}_b}(J(\bar{V}_b) + \frac{\omega}{2}\{\sum_{\beta(\ell^+)=b}|\bar{E}_{\ell+}^{k+1} - \bar{V}_b + \bar{\mu}_\ell^k|^2$$
$$+\sum_{\beta(\ell^-)=b}|\bar{E}_{\ell-}^{k+1} - \bar{V}_b + \bar{\nu}_\ell^k|^2\}) \tag{32}$$

3) Finally, dual variables, i.e., $\bar{\mu},\bar{\nu},\bar{\lambda}$ are updated:

$$\bar{\mu}_\ell^{k+1} = \bar{\mu}_\ell^k + (\bar{E}_{\ell+}^{k+1} - \bar{V}_{\beta(\ell^+)}^{k+1}) \tag{33}$$
$$\bar{\nu}_\ell^{k+1} = \bar{\nu}_\ell^k + (\bar{E}_{\ell-}^{k+1} - \bar{V}_{\beta(\ell^-)}^{k+1}) \tag{34}$$
$$\bar{\lambda}_g^{k+1} = \bar{\lambda}_g^k + (\bar{S}_g^{k+1} - \bar{z}_g^{k+1}) \tag{35}$$
$$\bar{\lambda}_c^{k+1} = \bar{\lambda}_c^k + (\bar{S}_c^{k+1} - \bar{z}_c^{k+1}) \tag{36}$$
$$\bar{\lambda}_{\ell+}^{k+1} = \bar{\lambda}_{\ell+}^k + (\bar{S}_{\ell+}^{k+1} - \bar{z}_{\ell+}^{k+1}) \tag{37}$$
$$\bar{\lambda}_{\ell-}^{k+1} = \bar{\lambda}_{\ell-}^k + (\bar{S}_{\ell-}^{k+1} - \bar{z}_{\ell-}^{k+1}) \tag{38}$$

The stopping criterion for this algorithm is that the primal and dual residuals (defined as in [45]) are less than a small predefined tolerance or that a maximum number of iterations has been reached.

In what follows, we show specific scenarios where the ADMM algorithm fails to converge to a solution.

B. Investigation of the Convergence of the ADMM-based Solution of the OPF Problem

We consider the same network in Fig. 3. Each network bus, apart from the slack bus, has a load and a generator connected to it. The demand in the network is assumed to be non-controllable, whereas the generators are assumed to be distributed solar panels with typical PV-type capability constraints. For this scenario, the capability limits and the values of loads and generation are given in Table V. In addition to the loads and generation, we consider that a shunt capacitor is connected to bus 2. In order to model this shunt capacitor, we consider that it is part of the first network line. In particular, we consider that the shunt capacitance on the sending end of the π-model of the line connecting buses 1 and 2 is modified accordingly to account for the shunt capacitor.

We implement and solve the ADMM algorithm in Matlab for two different cases that correspond to two different values

[6]In what follows we assume that demand is non-controllable. Also, as in [20] the constraints (3),(9) are considered internal constraints of the lines and devices respectively and $\bar{I}_\ell^+,\bar{I}_\ell^-$ are internal variables of the lines.

[7]Note that demand is not controllable, hence the loads do not require the solution of an optimization problem to update their power consumption.

Table V
PARAMETERS OF THE TEST NETWORK IN FIG.3 USED FOR THE ADMM-BASED SOLUTION OF THE OPF PROBLEM

Parameter	Value
Generators' power, $\lvert\bar{S}_{i_{g_{max}}}\rvert, i = 2, 3, 4$ (MVA)	$0.40, 0.39, 0.46$
Generators' power factor, $cos\phi_{i_g}, i = 2, 3, 4$	0.9
Loads' active power, $P_{i_c}, i = 2, 3, 4$ (MW)	$2.76, 2.16, 2.46$
Loads' reactive power, $Q_{i_c}, i = 2, 3, 4$ (MW)	$1.38, 1.08, 1.23$
Shunt capacitor (bus 2), case I and II (uF)	$(239, 859)$
Penalty term gain, ω	1
Tolerance and maximum number of iterations	$10^{-4}, 10^{4}$

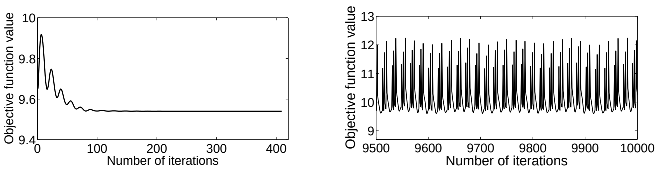

Fig. 7. Objective function value for case I and II (last 500 iterations).

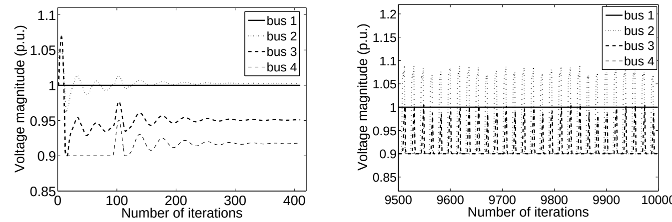

Fig. 8. Voltage magnitude evolution for cases I and II (last 500 iterations).

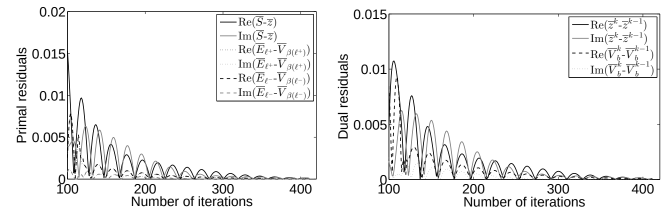

Fig. 9. Norm of the primal/dual residuals for case I (last 311 iterations).

of the size of the shunt capacitor (see Table V). In Case I, even though the OPF problem solved is the non-approximated non-convex one, ADMM converges, within the predefined tolerance, in 411 iterations. The left figure in Fig. 7 shows the objective function value as a function of the number of iterations of ADMM. The left figure in Fig. 8 shows the convergence of the buses' voltage magnitudes and Fig. 9 shows how the primal and dual residuals evolve with the iterations. On the contrary, in Case II, ADMM fails to converge to a solution and reaches the maximum number of iterations. This is shown in Fig. 7 (right), 8 (right) and 10 where the objective function, as well as the residuals and bus voltages are plotted for the last five hundred iterations until the maximum number of iterations is reached; we can observe that they exhibit oscillations.

In what follows we analyze why the ADMM algorithm converges in Case I but fails in Case II. To begin with, the first network line has the peculiarity that the voltage at its receiving end $\bar{E}_{\ell+}$ (i.e., the slack bus voltage) is fixed.[8] As a consequence, the first equality constraint in (26) becomes linear in the real and imaginary part of the voltage $\bar{E}_{\ell-}$, whereas the second equality constraint in (26) becomes quadratic on the real and imaginary part of the voltage $\bar{E}_{\ell-}$. In fact, the coefficients of the quadratic terms in the latter constraint are $Re(\bar{Y}_\ell)$ and $-Im(\bar{Y}_\ell) - Im(\bar{Y}_{\ell_0^-})$ for the real and imaginary parts, respectively. Due to the physics of the network, $Re(\bar{Y}_\ell)$ and $Im(\bar{Y}_{\ell_0^-})$ are positive for a network line and $Im(\bar{Y}_\ell)$ is negative. Furthermore, typically, the longitudinal reactance $Im(\bar{Y}_\ell)$ is much larger than the shunt capacitance $Im(\bar{Y}_{\ell_0^-})$ of a network line. Therefore, typically the coefficients of both quadratic terms are positive, and the line problem in (25) is convex for the lines that are connected to the slack bus. This is the case for the Case I. However, in Case II the size of the shunt capacitor, connected to bus 2, is such that $Im(\bar{Y}_{\ell_0^-}) > -Im(\bar{Y}_\ell)$, thus the coefficient of the aforementioned quadratic term in (26) is no longer positive and the corresponding line problem becomes non-convex.

Apart from the aforementioned case of the shunt capacitor, the ADMM algorithm also fails to converge to a solution when on-load tap changers (OLTCs) are included in the OPF formulation.[9] In fact, the effect of the OLTCs is similar to that of the shunt capacitors, in the sense that the line problem in (25) becomes once again non-convex for those lines that are connected to regulating transformers. To better understand why this occurs, let us consider a transformer with OLTC capabilities between buses 1 and 2 in the network and let us denote the ideal transformer admittance by Y_t and the OLTC ratio by α. Then based on the OLTC model in [46], the longitudinal admittance of the first network line equals αY_t and the shunt elements of the receiving and sending ends of the same line are $\alpha(\alpha-1)Y_t$ and $(1-\alpha)Y_t$ respectively. Hence, there is an additional control variable, namely the ratio α, that appears in the equality constraints (26) of the first network line problem, and both these constraints become quadratic in $\bar{E}_{\ell-}$ and α and non-convex.

V. CONCLUSION

In this first part of the paper we have focused on investigating the limits of the branch flow convexification proposed by Farivar-Low in [1,2] and of the ADMM-based solution of the OPF problem. In particular, we have discussed the misinterpretation of the physical model in the Farival-Low formulation

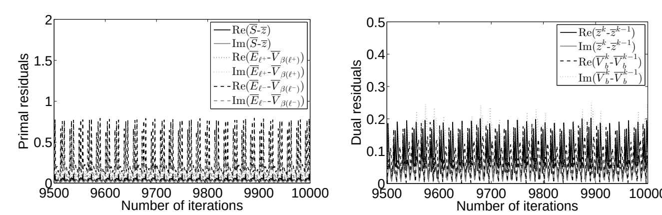

Fig. 10. Norm of the primal/dual residuals for case II (last 500 iterations).

[8]This holds for all the lines that are connected to the slack bus.

[9]For the sake of brevity we do not include the simulation results for this specific scenario.

of the OPF problem and the unrealistic assumptions therein. Finally, we have provided the ADMM-based decomposition of the OPF problem and we have shown, through specific examples, cases for which the ADMM-based solution of the non-relaxed OPF problem fails to converge.

References

[1] M. Farivar and S. H. Low, "Branch flow model: Relaxations and convexification - part I," *IEEE Trans. on Power Systems*, vol. 28, no. 3, pp. 2554–2564, 2013.

[2] M. Farivar and S. Low, "Branch flow model: Relaxations and convexification - part II," *IEEE Trans. on Power Systems*, vol. 28, no. 3, pp. 2565–2572, Aug 2013.

[3] J. Carpentier, "Contribution to the economic dispatch problem," *Bulletin de la Société Française des Electriciens*, vol. 3, no. 8, pp. 431–447, 1962.

[4] D. Sun, B. Ashley, B. Brewer, A. Hughes, and W. F. Tinney, "Optimal power flow by newton approach," *IEEE Trans. on Power Apparatus and Systems*, vol. PAS-103, no. 10, pp. 2864–2880, Oct 1984.

[5] D. Gayme and U. Topcu, "Optimal power flow with large-scale storage integration," *IEEE Trans. on Power Systems*, vol. 28, no. 2, pp. 709–717, May 2013.

[6] M. Adibi, R. Polyak, I. Griva, L. Mili, and S. Ammari, "Optimal transformer tap selection using modified barrier-augmented lagrangian method," *IEEE Trans. on Power Systems*, vol. 18, no. 1, pp. 251–257, Feb 2003.

[7] C. Lehmkoster, "Security constrained optimal power flow for an economical operation of FACTS-devices in liberalized energy markets," *IEEE Trans. on Power Delivery*, vol. 17, no. 2, pp. 603–608, Apr 2002.

[8] B. Hayes, I. Hernando-Gil, A. Collin, G. Harrison, and S. Djokić, "Optimal power flow for maximizing network benefits from demand-side management," *IEEE Trans. on Power Systems*, vol. 29, no. 4, pp. 1739–1747, July 2014.

[9] R. Jabr, "Optimal power flow using an extended conic quadratic formulation," *IEEE Trans. on Power Systems*, vol. 23, no. 3, pp. 1000–1008, Aug 2008.

[10] B. C. Lesieutre, I. Hiskens *et al.*, "Convexity of the set of feasible injections and revenue adequacy in FTR markets," *IEEE Trans. on Power Systems*, vol. 20, no. 4, pp. 1790–1798.

[11] I. A. Hiskens and R. J. Davy, "Exploring the power flow solution space boundary," *IEEE Trans. on Power Systems*, vol. 16, no. 3, pp. 389–395, 2001.

[12] Y. Makarov, Z.-Y. Dong, and D. Hill, "On convexity of power flow feasibility boundary," *IEEE Trans. on Power Systems*, vol. 23, no. 2, pp. 811–813, May 2008.

[13] J. A. Momoh, M. El-Hawary, and R. Adapa, "A review of selected optimal power flow literature to 1993. part I: Nonlinear and quadratic programming approaches," *IEEE Trans. on Power Systems*, vol. 14, no. 1, pp. 96–104, 1999.

[14] ——, "A review of selected optimal power flow literature to 1993. part II: Newton, linear programming and interior point methods," *IEEE Trans. on Power Systems*, vol. 14, no. 1, pp. 105–111, 1999.

[15] Z. Qiu, G. Deconinck, and R. Belmans, "A literature survey of optimal power flow problems in the electricity market context," in *Power Systems Conference and Exposition, PSCE. IEEE/PES*. IEEE, 2009, pp. 1–6.

[16] S. Bolognani, R. Carli, G. Cavraro, and S. Zampieri, "A distributed control strategy for optimal reactive power flow with power constraints," in *52nd Annual Conference on Decision and Control (CDC)*. IEEE, 2013, pp. 4644–4649.

[17] ——, "A distributed control strategy for optimal reactive power flow with power and voltage constraints," in *IEEE International Conference on Smart Grid Communications (SmartGridComm)*, Oct 2013, pp. 115–120.

[18] E. Dall'Anese, H. Zhu, and G. B. Giannakis, "Distributed optimal power flow for smart microgrids," *IEEE Trans. on Smart Grid*, vol. 4, no. 3, pp. 1464–1475, 2013.

[19] B. Zhang, A. Lam, A. Dominguez-Garcia, and D. Tse, "An optimal and distributed method for voltage regulation in power distribution systems," *IEEE Trans. on Power Systems*, vol. PP, no. 99, pp. 1–13, 2014.

[20] M. Kraning, E. Chu, J. Lavaei, and S. Boyd, "Dynamic network energy management via proximal message passing," *Foundations and Trends in Optimization*, vol. 1, no. 2, pp. 70–122, 2013.

[21] A. X. Sun, D. T. Phan, and S. Ghosh, "Fully decentralized AC optimal power flow algorithms," in *Power and Energy Society General Meeting (PES)*. IEEE, 2013, pp. 1–5.

[22] P. Sulc, S. Backhaus, and M. Chertkov, "Optimal distributed control of reactive power via the alternating direction method of multipliers," *IEEE Trans. on Energy Conversion*, vol. 29, no. 4, pp. 968–977, Dec 2014.

[23] Q. Peng and S. H. Low, "Distributed algorithm for optimal power flow on a radial network," *arXiv preprint arXiv:1404.0700*, 2014.

[24] T. Erseghe, "Distributed optimal power flow using ADMM," *IEEE Trans. on Power Systems*, vol. 29, no. 5, pp. 2370–2380, Sept 2014.

[25] A. G. Bakirtzis and P. N. Biskas, "A decentralized solution to the DC-OPF of interconnected power systems," *IEEE Trans. on Power Systems*, vol. 18, no. 3, pp. 1007–1013, 2003.

[26] B. Lesieutre, D. Molzahn, A. Borden, and C. Demarco, "Examining the limits of the application of semidefinite programming to power flow problems," in *2011 49th Annual Allerton Conference on Communication, Control, and Computing (Allerton)*, Sept 2011, pp. 1492–1499.

[27] D. P. Palomar and M. Chiang, "A tutorial on decomposition methods for network utility maximization," *IEEE Journal on Selected Areas in Communications*, vol. 24, no. 8, pp. 1439–1451, 2006.

[28] A. J. Conejo and J. A. Aguado, "Multi-area coordinated decentralized DC optimal power flow," *IEEE Trans. on Power Systems*, vol. 13, no. 4, pp. 1272–1278, 1998.

[29] P. N. Biskas, A. G. Bakirtzis, N. I. Macheras, and N. K. Pasialis, "A decentralized implementation of DC optimal power flow on a network of computers," *IEEE Trans. on Power Systems*, vol. 20, no. 1, pp. 25–33, 2005.

[30] O. Alsac, J. Bright, M. Prais, and B. Stott, "Further developments in LP-based optimal power flow," *IEEE Trans. on Power Systems*, vol. 5, no. 3, pp. 697–711, 1990.

[31] B. Stott and O. Alsaç, "Fast decoupled load flow," *IEEE Trans. on Power Apparatus and Systems*, no. 3, pp. 859–869, 1974.

[32] M. Baran and F. Wu, "Optimal sizing of capacitors placed on a radial distribution system," *IEEE Trans. on Power Delivery*, vol. 4, no. 1, pp. 735–743, Jan 1989.

[33] S. Bose, D. F. Gayme, K. M. Chandy, and S. H. Low, "Quadratically constrained quadratic programs on acyclic graphs with application to power flow," *arXiv preprint arXiv:1203.5599*, 2012.

[34] L. Gan and S. Low, "Convexification of AC optimal power flow," *PSCC*, Aug 2014.

[35] R. A. Jabr, "Radial distribution load flow using conic programming," *IEEE Trans. on Power Systems*, vol. 21, no. 3, pp. 1458–1459, 2006.

[36] J. Lavaei and S. Low, "Zero duality gap in optimal power flow problem," *IEEE Trans. on Power Systems*, vol. 27, no. 1, pp. 92–107, Feb 2012.

[37] M. Farivar, C. R. Clarke, S. H. Low, and K. M. Chandy, "Inverter VAR control for distribution systems with renewables," in *International Conference on Smart Grid Communications (SmartGridComm)*. IEEE, 2011, pp. 457–462.

[38] B. Stott, J. Jardim, and O. Alsaç, "DC power flow revisited," *IEEE Trans. on Power Systems*, vol. 24, no. 3, pp. 1290–1300, 2009.

[39] W. Bukhsh, A. Grothey, K. McKinnon, and P. Trodden, "Local solutions of the optimal power flow problem," *IEEE Trans. on Power Systems*, vol. 28, no. 4, pp. 4780–4788, Nov 2013.

[40] M. Farivar and S. H. Low, "Branch flow model: Relaxations and convexification." in *CDC*, 2012, pp. 3672–3679.

[41] N. Li, L. Chen, and S. H. Low, "Exact convex relaxation of OPF for radial networks using branch flow model." in *SmartGridComm*. Citeseer, 2012, pp. 7–12.

[42] L. Gan, N. Li, U. Topcu, and S. Low, "Branch flow model for radial networks: convex relaxation," in *Proceedings of the 51st IEEE Conference on Decision and Control*, 2012.

[43] R. Cespedes, "New method for the analysis of distribution networks," *IEEE Trans. on Power Delivery*, vol. 5, no. 1, pp. 391–396, Jan 1990.

[44] H.-D. Chiang and M. Baran, "On the existence and uniqueness of load flow solution for radial distribution power networks," *IEEE Trans. on Circuits and Systems*, vol. 37, no. 3, pp. 410–416, Mar 1990.

[45] S. Boyd, N. Parikh, E. Chu, B. Peleato, and J. Eckstein, "Distributed optimization and statistical learning via the alternating direction method of multipliers," *Foundations and Trends® in Machine Learning*, vol. 3, no. 1, pp. 1–122, 2011.

[46] W. D. Stevenson and J. J. Grainger, "Power system analysis," *New York: McGraw-Hill International Editions*, pp. 141–190, 1994.

AC OPF in Radial Distribution Networks - Part II: An Augmented Lagrangian-based OPF Algorithm, Distributable via Primal Decomposition

Konstantina Christakou, *Member, IEEE*, Dan-Cristian Tomozei, *Member, IEEE*, Jean-Yves Le Boudec, *Fellow, IEEE*, Mario Paolone, *Senior Member, IEEE*

***Abstract*—In the first part of this two-part paper we show that the branch-flow convexification of the OPF problem is not exact and that the ADMM-based decomposition of the OPF fails to converge in specific scenarios. Therefore, there is a need to develop algorithms for the solution of the non-approximated OPF problem that remains inherently non-convex. To overcome the limitations of recent approaches for the solution of the OPF problem, we propose in this paper, a specific algorithm for the solution of a non-approximated, non-convex AC OPF problem in radial distribution systems. It is based on the method of multipliers, as well as on a primal decomposition of the OPF problem. We provide a centralized version, as well as a distributed asynchronous version of the algorithm. We show that the centralized OPF algorithm converges to a local minimum of the global OPF problem and that the distributed version of the algorithm converges to the same solution as the centralized one. Here, in this second part of the two-part paper, we provide the formulation of the proposed algorithm and we evaluate its performance by using both small-scale electrical networks, as well as a modified IEEE 13-node test feeder.**

***Index Terms*—OPF, ADMM, decomposition methods, method of multipliers, convex relaxation, active distribution networks, distributed algorithms, asynchronous algorithms.**

I. Introduction

In Part I of this two-part paper we present the generic formulation of the non-convex OPF problem and we briefly review several OPF algorithms that are based on approximations and assumptions in order to guarantee convergence. Furthermore, we focus on the branch-flow convexification of the OPF problem that has been recently proposed by Farivar and Low in [1,2] and is claimed to be exact for the case of radial distribution systems under specific assumptions, despite the absence of apparent approximations. We show that this claim, in fact, does not hold, as it leads to an incorrect system model and therefore, there is a need to develop algorithms for the solution of the non-approximated OPF problem that remains inherently non-convex. In detail, we show through practical examples that in [1,2], on one hand, there is a misinterpretation of the physical network model related to the ampacity constraint of the lines' current flows and, on the other hand, the proof of the exactness of the proposed relaxation requires unrealistic assumptions related to the unboundedness of specific control variables. Furthermore, we investigate the application of ADMM for the solution of the original non-approximated OPF problem. Even though ADMM requires the underlying problem to be convex in order to guarantee convergence, it was applied also to the case of non-convex AC OPF problems with promising convergence performance (e.g., [3,4]). However, we show, through practical examples, cases for which the ADMM-based decomposition of the non-relaxed OPF problem fails to converge.

To overcome the aforementioned limitations, here in this second part, we propose an algorithm for the solution of the non-approximated non-convex AC OPF problem in radial networks. Our proposed solution uses an augmented Lagrangian approach and relies on the method of multipliers ([5]–[7]). In particular, we design a centralized OPF algorithm that is proven to converge to a local minimum of the original non-approximated OPF problem.

With respect to the case of controlling multiple dispersed energy resources, it is of interest to also define a distributed solution method that is formally equivalent to the centralized formulation. In fact, several distributed OPF algorithms are proposed in the literature. In [8,9] the authors design a dual-ascent algorithm for optimal reactive power flow with power and voltage constraints. In [10,11] dual decomposition is used as the basis for the distributed solution of the OPF problem. Finally, a significant number of contributions propose distributed formulations of the OPF problem, based on the alternating direction method of multipliers (ADMM) (e.g., [3,4,10,12]–[14]).

In this direction, we present, here in this second part, a distributed version of the proposed algorithm that, unlike ADMM, is based on a primal decomposition [15] and does not require that the problem be convex. In this decentralized version of the algorithm, at each iteration, local agents, assigned to network buses and network lines, exchange messages with their neighbors using only local information. We prove that the distributed algorithm converges to the same solution as the centralized version. Finally, we present an asynchronous implementation of the distributed algorithm where the messages of the neighboring agents need not be synchronized.

The structure of this second part is the following. In Section II we describe the proposed algorithm for the OPF solution. We present both a centralized, as well as a decentralized asynchronous version of the proposed algorithm. In Section III we investigate the convergence of the proposed algorithm in the cases where the BFM convexification leads to an incorrect solution and ADMM fails to converge to a solution. In Section

Konstantina Christakou, Dan-Cristian Tomozei, Jean-Yves Le Boudec and Mario Paolone (email: konstantina.christakou@epfl.ch, dan-cristian.tomozei @epfl.ch, jean-yves.leboudec@epfl.ch, mario.paolone@epfl.ch) are with the École Polytechnique Fédérale de Lausanne, CH-1015 Lausanne, Switzerland.

IV we evaluate the performance of the proposed algorithm using a modified IEEE 13-node test feeder. Finally, in Section V we provide the main observations and concluding remarks for this Part II.

II. AC OPF IN RADIAL DISTRIBUTION SYSTEMS

We first write the AC OPF problem presented in Part I in an equivalent form, and then we provide a centralized, as well as a distributed algorithm for its resolution.

We make the following assumptions about the grid model:

A1. We consider a direct sequence representation of the grid;
A2. Any two-port component (e.g., lines, transformers etc.) is represented as a π-equivalent;
A3. We assume a perfect knowledge of the system parameters, i.e., the network admittance matrix is known;
A4. The nodal-power injections are voltage-independent;
A5. The control variables are composed by the nodal power injections/absorptions.

A. The Proposed Centralized OPF Algorithm

We are interested in maximizing the social welfare of the economic agents that use the grid, while maintaining an acceptable network voltage profile and respecting the line ampacity limits. Specifically, we tune the line ampacities and the network voltage profiles by controlling the (P, Q)-injections of distributed controllable devices $\mathcal{G}$ (*e.g.*, renewable generators) in a "fair" way: Each controllable device $g \in \mathcal{G}$ has a certain utility function $U_g(\cdot)$, and the sum of these utility functions is maximized subject to the satisfaction of the network operation constraints (voltage and ampacity). The resulting set-point is thus Pareto-optimal, *i.e.*, no single device can increase its utility without hurting the utility of some other device, and locally-"fair", *i.e.*, the resulting set-point is a local maximizer of the sum of the device utilities lying on the Pareto boundary of feasible set-points.

By convention, each line $\ell \in \mathcal{L}$ has a "receiving" and a "sending" end, which we denote by ℓ^+ and ℓ^-, respectively. These are chosen arbitrarily. A line is connected to two adjacent buses to which we refer by $\beta(\ell^+)$ and $\beta(\ell^-)$, respectively. For each line, we introduce two auxiliary variables $\bar{E}_{\ell^+}$ and $\bar{E}_{\ell^-}$ representing the complex voltage at the two ends of the line. Assumptions A1-A3 allow us to express the corresponding injected currents and powers at the two ends of line ℓ:

$$\bar{I}_{\ell^+} = \bar{I}_{\ell^+}(\bar{E}_{\ell^+}, \bar{E}_{\ell^-}) = (\bar{Y}_\ell + \bar{Y}_{\ell_0^+})\bar{E}_{\ell^+} - \bar{Y}_\ell \bar{E}_{\ell^-} \tag{1}$$

$$\bar{I}_{\ell^-} = \bar{I}_{\ell^-}(\bar{E}_{\ell^+}, \bar{E}_{\ell^-}) = (\bar{Y}_\ell + \bar{Y}_{\ell_0^-})\bar{E}_{\ell^-} - \bar{Y}_\ell \bar{E}_{\ell^+} \tag{2}$$

$$\bar{S}_{\ell^+} = \bar{S}_{\ell^+}(\bar{E}_{\ell^+}, \bar{E}_{\ell^-}) = \bar{E}_{\ell^+} \underline{I}_{\ell^+} \tag{3}$$

$$\bar{S}_{\ell^-} = \bar{S}_{\ell^-}(\bar{E}_{\ell^+}, \bar{E}_{\ell^-}) = \bar{E}_{\ell^-} \underline{I}_{\ell^-} \tag{4}$$

In the remainder of this paper, unless otherwise stated, the complex line currents and powers expressed above are always computed according to equations (1)-(4). They are thus all functions of $\bar{E}_{\ell^+}$ and $\bar{E}_{\ell^-}$ *exclusively*, although the arguments are often omitted for the sake of brevity. All quantities are expressed in "per-unit", unless otherwise specified.

For readability, we denote the vector formed by the real and imaginary parts of variables $(\bar{E}_{\ell^+}, \bar{E}_{\ell^-})_\ell$ by $y \in \mathbb{R}^{4L}$, where $L = |\mathcal{L}|$ is the number of lines. Note that for a given value of y, the corresponding currents and powers do not necessarily satisfy Kirchhoff's law.

We call y feasible if it satisfies voltage consistency and per-bus power-balance. Voltage consistency means that the voltages of all the lines incident to a specific bus $b \in \mathcal{B}$ are identical, *i.e.*, have the same amplitude V_b and the same argument φ_b:

$$|\bar{E}_{\ell^+}| = V_{\beta(\ell^+)}, \quad |\bar{E}_{\ell^-}| = V_{\beta(\ell^-)} \tag{5}$$

$$\arg(\bar{E}_{\ell^+}) = \varphi_{\beta(\ell^+)}, \quad \arg(\bar{E}_{\ell^-}) = \varphi_{\beta(\ell^-)}, \quad \forall \ell \in \mathcal{L}. \tag{6}$$

At each bus $b \in \mathcal{B}$, power-balance is satisfied if and only if

$$\sum_{\beta(\ell^+)=b} \bar{S}_{\ell^+} + \sum_{\beta(\ell^-)=b} \bar{S}_{\ell^-} = -\sum_{g \in b} \bar{S}_g - \bar{S}(b), \quad \forall b \in \mathcal{B}, \tag{7}$$

where S_g is the controlled generated power of device g found at bus b, $\bar{S}(b)$ denotes the non-controllable power injection at bus b, and $\bar{S}_{\ell^+}$, $\bar{S}_{\ell^-}$ are obtained via (3)-(4).

If y is feasible, it is important to note that equations (1)-(4) describe the exact AC power-flow equations. Hence, we use a non-approximated model of the grid.

We write the OPF formulation (Part I) equivalently:[1]

$$\max_{\substack{\bar{S}_g, V_b, \varphi_b \\ \bar{E}_{\ell^+}, \bar{E}_{\ell^-}}} \sum_{g \in \mathcal{G}} W_g(\bar{S}_g) \qquad \text{subject to:} \tag{8}$$

Feasibility constraints (5), (6), (7)

$$|\bar{I}_{\ell^+}| \le I_{\ell,\max} \text{ and } |\bar{I}_{\ell^-}| \le I_{\ell,\max}, \qquad \forall \ell \in \mathcal{L} \tag{9}$$

$$V_{\min} \le V_b \le V_{\max}, \qquad \forall b \in \mathcal{B} \tag{10}$$

$$\bar{S}_g \in \mathcal{H}_g, \qquad \forall g \in \mathcal{G} \tag{11}$$

As previously stated, the objective function is the sum of the welfare of the controllable devices W_g. In the above formulation, we denote by $\mathcal{G}$ the set of controllable devices and by $\bar{S}_g = P_g + jQ_q$ the controllable injected power by device g, subject to the capability constraint (11). The set $\mathcal{G}$ can contain both generators and consumers. However, for the sake of presentation clarity, we consider that $\mathcal{G}$ contains uniquely PV generators. This is not a limiting assumption, as our results apply to any device with controllable power injections (including controllable loads). Non-controllable loads do not appear in the objective function, that expresses the utility of PV generators (a concave increasing function $U(\cdot)$ of active power injection) and the losses of the power converter:

$$W_g(\bar{S}_g) = U_g(P_g) - \eta(P_g^2 + Q_g^2), \ \forall g \in \mathcal{G}. \tag{12}$$

We consider typical capability curves of PV power inverters:

$$\mathcal{H}_g = \{\bar{S}_g : |\bar{S}_g| \le S_{g,\max}, \ |arg(\bar{S}_g)| \le \phi_{g,\max}\}. \tag{13}$$

In order to solve the problem (8)-(11), we convert the inequality constraints (9) to equality constraints by introducing slack variables i_{ℓ^+} and i_{ℓ^-} as follows:

$$|\bar{I}_{\ell^+}| + i_{\ell^+} = I_{\ell,\max} \text{ and } |\bar{I}_{\ell^-}| + i_{\ell^-} = I_{\ell,\max}, \forall \ell \in \mathcal{L} \tag{14}$$

$$i_{\ell^+}, i_{\ell^-} \ge 0, \quad \forall \ell \in \mathcal{L} \tag{15}$$

[1]Unlike in Part I, we consider wlog that there are two types of connected devices: they either have controllable power injection $\bar{S}_g$ or impose an overall fixed power injection $\bar{S}(b)$ in bus b.

We denote by x the real vector of variables formed by the artificial control variables $(V_b, \varphi_b)_{b\in\mathcal{B}}$, $(i_{\ell+}, i_{\ell-})_{\ell\in\mathcal{L}}$, and the device controllable injected power $(P_g, Q_g)_{g\in\mathcal{G}}$.

Notice that all the equality constraints above, (5), (6), (7), and (14) can be summarized as $g(y) + Ax + b = 0$, where $g(\cdot)$ is a smooth non-convex function that can be derived from equations (1)-(6), and A is a positive definite matrix. Similarly, the inequality constraints, (10), (11), and (15), can be expressed as $h(x) \geq 0$, where $h(x)$ is a convex function that can be derived from equations (10), (15), and (13). We denote the objective by $f(x)$, where f is concave.

We can thus write our problem in the more compact form:

$$\max_{x,y} f(x) \tag{16}$$

$$\text{subject to } g(y) + Ax + b = 0 \tag{17}$$

$$h(x) \geq 0. \tag{18}$$

We write its augmented Lagrangian ([5]–[7]):

$$\mathcal{L}_\rho(x, y; \lambda) = f(x) + \lambda'(g(y) + Ax + b) - \frac{\rho}{2}\|g(y) + Ax + b\|^2, \tag{19}$$

where ρ is the weight of the quadratic penalty term added to the classic Lagrangian function, and λ is the vector of Lagrange multipliers associated with the equality constraints (17).

Our centralized iterative algorithm for solving the OPF is based on the method of multipliers ([5, §4.2]). This method was first introduced for solving iteratively non-linear equality constrained problems. It is shown to converge under more general conditions than dual ascent [16]. Algorithm 1 summarizes the proposed centralized algorithm, and Theorem 1 characterizes its convergence.

Algorithm 1 Centralized algorithm for the OPF (16)-(18)

- Set k=0 and initialize control variables x and y: $\bar{S}_g^0 = 0, \bar{E}_{\ell+}^0 = \bar{E}_{\ell-}^0 = 1, V_b^0 = 1, \varphi_b^0 = 0, i_{\ell+}^0 = i_{\ell-}^0 = 0$ (per-unit), Lagrange multipliers $\lambda^0 = 0$, increasing gain sequence $(\rho^k)_k$, $\rho^k \to \infty$.

repeat

Maximize the augmented Lagrangian for fixed $\lambda = \lambda^k$:

$$(x^{k+1}, y^{k+1}) = \underset{x,y:h(x)\geq 0}{\arg\max}\, L_{\rho^k}(x, y; \lambda^k). \tag{20}$$

Update the Lagrange multipliers:

$$\lambda^{k+1} = \Pi_{[-\bar{\lambda},\bar{\lambda}]}\left\{\lambda^k + \rho^k\left[g(y^{k+1}) + Ax^{k+1} + b\right]\right\} \tag{21}$$

$k \leftarrow k+1$

until the maximum number of iterations has been reached **or** the change in the Lagrange multipliers between two consecutive iterations is less than a tolerance $\delta > 0$

The main advantage of the method of multipliers is that there exists a finite value $\bar{\rho}$ such that the problem (20) is convex for all $\rho^k > \bar{\rho}$. Note also that the algorithm bounds the value of λ at each iteration. The next vector of multiplier estimates λ is obtained after a projection on the set $[-\bar{\lambda}, \bar{\lambda}]$ defined as $[-\bar{\lambda}_1, \bar{\lambda}_1] \times [-\bar{\lambda}_2, \bar{\lambda}_2] \times \ldots$; the constant vector $\bar{\lambda}$ is chosen such that the sought optimal vector of Lagrange multipliers λ^* lies in $[-\bar{\lambda}, \bar{\lambda}]$ (see [17, §2.2.2]).

Theorem 1: For smooth objective function $f \in \mathcal{C}^2$ and suitably chosen $\bar{\lambda}$ such that the optimal vector of Lagrange multipliers λ^* satisfies $\lambda^* \in [-\bar{\lambda}, \bar{\lambda}]$, Algorithm 1 converges to a local minimum of the nonlinear progam (16)-(18).

Proof: By [17, Proposition 1.23], our problem satisfies assumption (S) from [17, §2.2], since the equality constraint is a $\mathcal{C}^2$ function of y, and the objective function is chosen to be $\mathcal{C}^2$. Proposition 2.7 from the same reference guarantees the desired convergence, if the iterates (x^k, y^k, λ^k) reach the set D from Proposition 2.4 of [17], *i.e.*, if there exists a $\bar{k}$ such that $(x^{\bar{k}}, y^{\bar{k}}, \lambda^{\bar{k}}) \in D$ (for all the following indices $k > \bar{k}$, the iterates stay in D, and convergence ensues). The existence of such a $\bar{k}$ follows from the choice of the divergent increasing sequence of gains (ρ^k) and from the boundedness of the sequence (λ^k). ■

Due to the quadratic terms in the expression of the augmented Lagrangian (19), the optimization problem in (20) does not decouple across the network and, therefore, cannot be solved in a distributed manner. In the following section, we reformulate this problem in an equivalent way that leads to a distributed algorithm for its resolution.

B. Distributed Solution of the OPF Problem

We adopt a primal decomposition method [15] that gives an iterative algorithm for the minimization of the problem in *Step 2* of Algorithm 1. In (19) the line voltages $y = (\bar{E}_{\ell+}, \bar{E}_{\ell-})$ are "coupling" variables. If these variables are fixed to a specific value, then problem (20) decouples in smaller, easier (convex) problems, that can be solved by local agents.

Specifically, to solve (20) iteratively for fixed values of the Lagrange multiplier estimates $\hat{\lambda}$ and fixed gain $\hat{\rho}$ we take the following approach: At the n-th iteration, the value of the coupling variables $y^n = (\bar{E}_{\ell+}^n, \bar{E}_{\ell-}^n)$ is assumed fixed. The x variables, *i.e.*, the power set-points of the controllable devices $(\bar{S}_g)$, the bus voltages $(\bar{V}_b)$, and the slack variables $i_{\ell+}, i_{\ell-}$, are computed by solving the following constrained convex optimization problem:

$$x^{n+1} = \underset{x:h(x)\geq 0}{\arg\max}\, L_{\hat{\rho}}(x, y^n, \hat{\lambda}). \tag{22}$$

Next, the coupling variables y are updated as follows:

$$y^{n+1} = y^n + \alpha^n(\nabla_y L_{\hat{\rho}})(x^{n+1}, y^n, \hat{\lambda}), \tag{23}$$

where α^n is a positive step-size sequence of the gradient descent. The choice of the step-size is related to the topology of the network and the parameters of the lines (i.e., the network admittance matrix). For example, a large constant step-size might not allow the algorithm to converge, whereas a small constant step-size could cause slow convergence[2].

[2]In order to properly tune this parameter, a dedicated off-line study can be performed before deployment of the proposed algorithm.

The algorithm stops when the norm of the update in the y variables is less than some small positive tolerance ε, *i.e.*, when $\|\nabla_y L_{\hat{\rho}}(x^{n+1}, y^n, \hat{\lambda})\| \le \varepsilon$.

Theorem 2: The algorithm (22)-(23) with tolerance ε in the stopping criterion converges to a vicinity $\mathcal{B}((x^*, y^*), \delta)$ of a local optimum (x^*, y^*) of problem (20). If (20) is strongly locally convex in y in a vicinity of (x^*, y^*), then $\delta = \Theta(\varepsilon^2)$.

Proof: (Sketch) Denote $v(y) = \max_{x:h(x)\ge 0} L_{\hat{\rho}}(x, y, \hat{\lambda})$ and $x^*(y)$ the value of x that achieves this maximum (22). Theorem 2.1 of [18] says that the optimum $(x^*(y^*), y^*)$ of $\max_y v(y)$ coincides with the one of (20). Moreover, a δ-optimal solution $(x^*(y_\delta), y_\delta)$ of $\max_y v(y)$ (that is, $v(y_\delta) \ge v(y^*) - \delta$) is also δ-optimal for (20).

We now show that $\nabla_y v(y) = (\nabla_y L_{\hat{\rho}})(x^*(y), y, \hat{\lambda})$, or equivalently, $\frac{Dx^*(y)}{Dy}(\nabla_x L_{\hat{\rho}})(x^*(\bar{y}), \bar{y}, \hat{\lambda}) = 0$. If we can show this, then the algorithm (22)-(23) is equivalent to a gradient ascent in y on $v(y)$. It is easy to show that the function $v(y)$ is "smooth" ($\mathcal{C}^2$). By the strong local convexity around (x^*, y^*) of the augmented Lagrangian, [5, Exercise 1.2.10] allows us to conclude that $\delta = \Theta(\varepsilon^2)$.

Note that problem (22) is convex. Consider the optimal multipliers μ^* corresponding to the constraints $h(x) \ge 0$. They satisfy the KKT conditions:

$$(\nabla_x L_{\hat{\rho}})(x^*(y), y, \hat{\lambda}) = \sum_i \mu_i^*(y) \nabla_x h_i(x^*(y))$$
$$\mu_i^*(y) h_i(x^*(y)) = 0; \quad \mu_i^* \ge 0.$$

Define the following functions: $\psi_i(y) := h_i(x^*(y))$. Since $x^*(y)$ is always feasible, it means that $\psi_i(y) \ge 0$. Consider the set of indices $\mathcal{I}_0(y) := \{i : h_i(x^*(y)) = 0\}$. Take some $i \in \mathcal{I}_0(y)$. In this case the function $\psi_i(y)$ has an extremal point in y, which implies that $\nabla_y \psi_i(y) = 0$, or again that $\frac{Dx^*(y)}{Dy}\nabla_x h_i(x^*(y)) = 0$. For all $i \notin \mathcal{I}_0(y)$, by KKT we have $\mu_i^*(y) = 0$. By the above arguments,

$$\begin{aligned}&\frac{Dx^*(y)}{Dy}(\nabla_x L_{\hat{\rho}})(x^*(y), y, \hat{\lambda}) \\ &= \sum_i \mu_i^*(y) \frac{Dx^*(y)}{Dy} \nabla_x h_i(x^*(y)) = 0.\end{aligned}$$

■

Thanks to its separability property, problem (22) can be solved in a distributed manner. Bus agents can be responsible for updating the power set-points of the controllable devices ($\bar{S}_g$) that are connected to them, as well as their voltages ($\bar{V}_b$) in parallel, and lines can be responsible for updating the slack variables ($i_{\ell+}, i_{\ell-}$). Specifically, the 'power set-points ($\bar{S}_g^{n+1}$) of devices in bus b are obtained by solving the following convex problem:

$$\begin{aligned}(\bar{S}_g^{n+1}) = &\arg\max_{\bar{S}_g \in \mathcal{H}_g} \sum_{g\in b} W_g(\bar{S}_g) \\ &- \frac{\hat{\rho}}{2}\Big| \sum_{g\in b} \bar{S}_g + \bar{S}(b) + \sum_{\beta(\ell^+)=b} \bar{S}_{\ell+}^n + \sum_{\beta(\ell^-)=b} \bar{S}_{\ell-}^n - \frac{\hat{\lambda}_b}{\hat{\rho}}\Big|^2,\end{aligned}$$

where $\hat{\lambda}_b$ is the given multiplier corresponding to the constraint (7) of bus b. The other problems (for the other x variables) have simpler expressions that we do not reproduce for brevity sake.

Similarly, (23) can be decomposed across the different network lines: line-agents can update the voltages at their two ends in parallel. In terms of required information, each bus agent needs to know only the voltage values of the lines that are incident to it, the constraints of the devices, and the state of the loads that are connected to it. Finally, in order to compute the partial derivatives of (23) with respect to its voltages, each line requires solely the information of the power balance and the voltage values of its two adjacent buses. The actual implementation of the distributed synchronous OPF algorithm is summarized below in Algorithm 2.

Algorithm 2 Distributed algorithm for the OPF (16)-(18)

- Set k=0 and initialize control variables x and y: $\bar{S}_g^0 = 0, \bar{E}_{\ell+}^0 = \bar{E}_{\ell-}^0 = 1, V_b^0 = 1, \varphi_b^0 = 0, i_{\ell+}^0 = i_{\ell-}^0 = 0$ (per-unit), Lagrange multipliers $\lambda^0 = 0$, increasing diverging gain sequence $(\rho^k)_k$, $\rho^k \to \infty$, decreasing tolerance sequence $(\varepsilon^k \ge 0)_k$, $\varepsilon^k \to 0$.

repeat
  $n \leftarrow 0$; $\tilde{x}^0 \leftarrow x^k$; $\tilde{y}^0 \leftarrow y^k$
  repeat
    $\tilde{x}^{n+1} = \arg\max_{x:h(x)\ge 0} L_{\rho^k}(x, \tilde{y}^n, \lambda^k)$
    $\tilde{y}^{n+1} = \tilde{y}^n + \alpha^n(\nabla_y L_{\rho^k})(\tilde{x}^{n+1}, \tilde{y}^n, \lambda^k)$
    $n \leftarrow n+1$
  until $\|\nabla_y L_{\rho^k}(\tilde{x}^{n+1}, \tilde{y}^n, \lambda^k)\| \le \varepsilon^k$
  $x^{k+1} \leftarrow \tilde{x}^{n+1}$; $y^{k+1} \leftarrow \tilde{y}^{n+1}$
  $\lambda^{k+1} = \Pi_{[-\bar{\lambda}, \bar{\lambda}]}\left\{\lambda^k + \rho^k\left[g(y^{k+1}) + Ax^{k+1} + b\right]\right\}$
  $k \leftarrow k+1$
until the maximum number of iterations has been reached **or** the change in the Lagrange multipliers between two consecutive iterations is less than a tolerance $\delta > 0$

Theorem 3: For smooth objective function $f \in \mathcal{C}^2$ and suitably chosen $\bar{\lambda}$ such that the optimal vector of Lagrange multipliers λ^* satisfies $\lambda^* \in [-\bar{\lambda}, \bar{\lambda}]$, Algorithm 2 converges to a local minimum of the nonlinear progam (16).

Proof: The proof is similar to the one of Theorem 1. It uses Proposition 2.16 of [17] for convergence, which only requires at each iteration a δ^k-optimal solution for (20) with $\delta^k \to 0$. By Theorem 2 we can conclude. ■

In a realistic setting, in order to take full advantage of the distributed formulation of the OPF algorithm, as described above and to avoid the overhead cost of coordination between agents, the updates should be performed in an asynchronous fashion. Contrary to ADMM-based algorithms, which require a synchronized implementation of the updates, the proposed algorithm can be implemented in an asynchronous manner. In this direction, we assume that each of the bus and line agents has its own two local poisson clocks with different rates. The clock with the lower rate ($C1$) triggers the multiplier update (21) and the clock with the higher rate ($C2$) triggers the events described in steps (22)-(23).

In detail, all the control variables and the Lagrange multipliers are first initialized. Then, every time the $C2$ clock of a bus ticks, this bus performs local update operations by using the most recent stored values for the voltages of its incident lines and for the associated Lagrange multipliers. Once the bus updates its power and voltage values, it informs the incident lines of the changes. Similarly, when the $C2$ clock of a line ticks, the line agent updates the variables $(i_{\ell+}, i_{\ell-})$ by taking into account the most recent values of the line current flows and associated Lagrange multipliers. In addition to this update, the updates of the voltages of its two end-points are triggered. In order to compute the new values, the line uses the most recent stored values for the adjacent buses' powers and voltages, and once the updates are completed the line communicates this information to its neighboring buses. Now, when the $C1$ clock of a bus or a line ticks, then the corresponding agent updates the Lagrange multipliers (21). It is worth noting, that we no longer have a serial implementation of the various updates like the ones presented in Algorithm 2. On the contrary, the different rates of the clocks are chosen in such a way to ensure that, on average, a sufficient number of the updates occurs before an update of the corresponding Lagrange multiplier takes place.

III. Performance Evaluation of the Centralized OPF Algorithm

In this section, we investigate the performances and convergence properties of the centralized Algorithm 1 in several different scenarios. In particular, we consider the cases presented in Part I of the paper, where the BFM convexification leads to an incorrect solution of the OPF problem and ADMM fails to converge to a solution. Additionally, we investigate the performances of the proposed centralized algorithm under different initial conditions of the electrical-network state. In order to do so, we consider the same 4-bus test network that was used in Part I of the paper. We assume a first test case where the controllable device connected to bus 4 is a generator, whereas controllable loads are connected to buses 2 and 3. The network characteristics, the base values, the capability limits of the controllable resources, and the voltage and ampacity limits are given in Part I (Fig. 3 and Table II). In what follows, the objective function accounts for the minimization of the network losses, as well as for the utility of the generating units, namely:

$$\min_{\bar{S}_g, \bar{S}_\ell, V_b, \varphi_b, |\bar{I}_\ell|} -\sum_{g \in \mathcal{G}} Re(\bar{S}_g) + \sum_{\ell \in \mathcal{L}} Re(\bar{Y}_\ell)|\bar{I}_\ell|^2 \qquad (24)$$

A. Effect of the Line Length, Network Rated Value and Network State on the Convergence of Algorithm 1

In order to compare the performances of the proposed algorithm with the OPF algorithm proposed in [1,2], we solve the OPF problem for various line lengths and network voltage rated values as in Part I of the paper. In particular, we assume that the line lengths are uniformly multiplied by a factor in the range $[1.25 - 7.5]$ (while keeping the network voltage rated value to its nominal value) and the network voltage rated value varies in the range $[15 - 40]kV$ (while keeping the line lengths to their nominal values). The evolution of the bus voltages, the line-current flows, as well as the active and reactive powers, are shown in Figures 1-6. It is worth

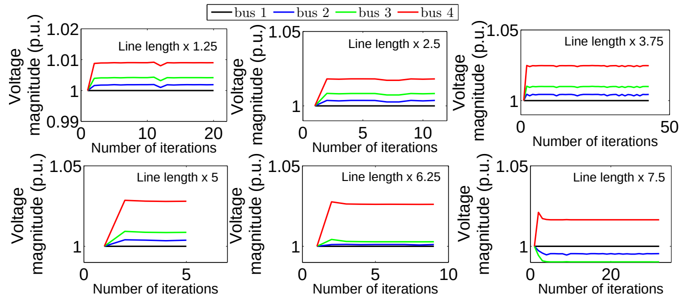

Fig. 1. Evolution of the magnitude of network voltages for various line lengths.

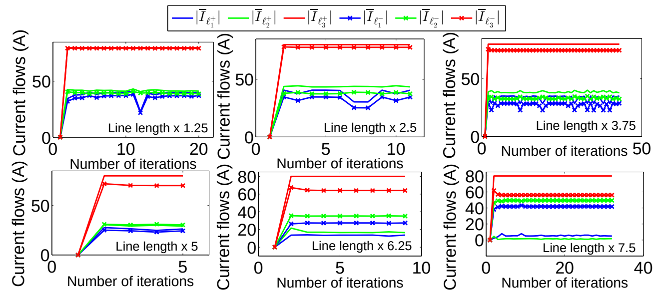

Fig. 2. Evolution of the line current flows for various line lengths.

noting that in all the cases the proposed algorithm converges in a few iterations. Furthermore, we observe from Fig. 2 and Fig. 5 that the line-current flows satisfy the line ampacity limit, once the algorithm has converged, in all cases. In particular, in Fig. 2 it is worth observing that as the line length increases the receiving and sending-end current flows of the same line become significantly different. The behavior of the current flows as the voltage rated value increases is similar (Fig. 5). This effect is due to the increasing contribution of the current flow toward the shunt elements of the lines. In fact, we show, in Figures 7 and 8, the amount of reactive power produced by the shunt elements of the lines for the various values of the line lengths and the network voltage rated values. We observe that as the line length increases or the rated value of the voltage increases the reactive power produced by the shunt elements of the line increases as well.

We investigate, in addition to the effect of the line lengths and the network voltage rated value, the performance of the proposed algorithm under a different network operating point. To this end, we consider a second test-case where the controllable device connected to bus 4 is a controllable load and generators are connected to buses 2 and 3. In this respect, we consider an extra term in the objective function, which represents the utility associated with the controllable load and is given by $(P_L - P_o)^2$, where P_o represents a constant amount of load that has to be served. The capability limits of the controllable resources are shown in Table I. The convergence of the voltages, current flows, as well as active and reactive powers are shown in Fig. 9. For the sake of brevity, we only show the evolution of the active and reactive power of the controllable load of bus 4, as the controllable generators are small and reach their maximum value upon convergence.

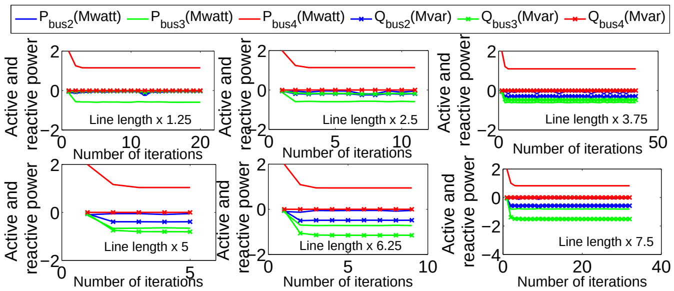

Fig. 3. Evolution of the active and reactive power of the controllable devices for various line lengths.

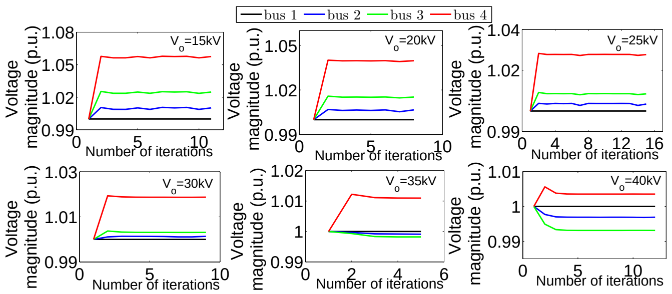

Fig. 4. Evolution of the magnitude of network voltages for various values of the network rated voltage.

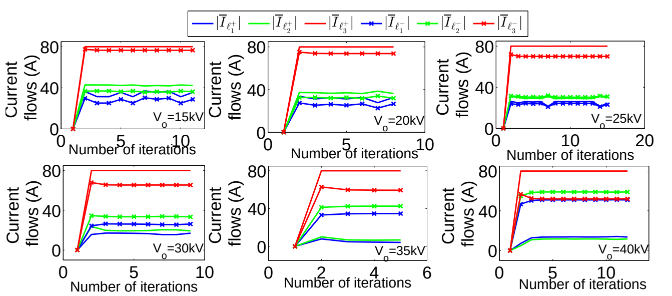

Fig. 5. Evolution of the line current flows for various values of the network rated voltage.

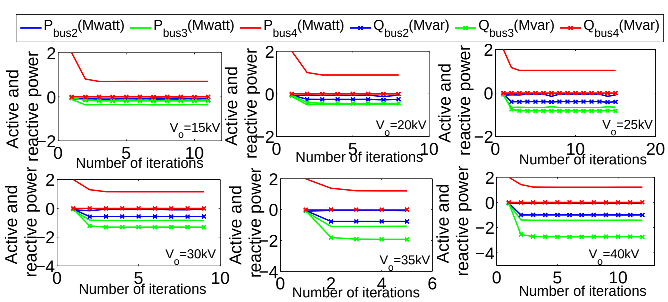

Fig. 6. Evolution of the magnitude of active and reactive power of the controllable devices for various values of the network rated voltage.

Table I
PARAMETERS OF THE TEST NETWORK USED FOR THE INVESTIGATION OF THE PERFORMANCE OF THE PROPOSED OPF ALGORITHM UNDER A DIFFERENT OPERATING POINT

Parameter	value
$[P_{g_{min}}, P_{g_{max}}]$(bus 2) (MW)	$[0, 0.01]$
$[P_{g_{min}}, P_{g_{max}}]$(bus 3) (MW)	$[0, 0.012]$
$(P_{c_{min}}, Q_{c_{min}})$(MW,Mvar) (bus 4)	0.3, 0.15
P_o(MW) (bus 4)	1

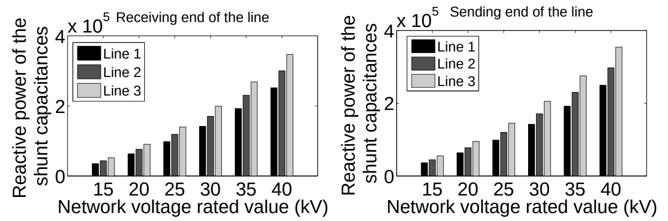

Fig. 7. Reactive power produced by the shunt elements of the lines for various values of the network voltage rated value.

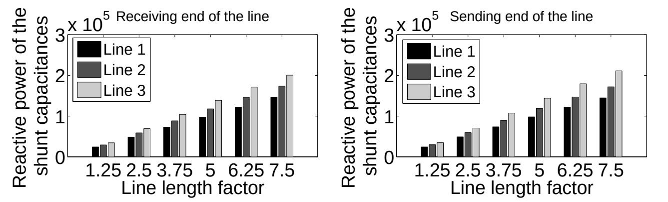

Fig. 8. Reactive power produced by the shunt elements of the lines for various line lengths.

B. Performance Evaluation of the Proposed Algorithm in the Presence of Shunt Capacitors in the Network

In what follows, we consider the same network adopted in the previous section and a case where each network bus, apart from the slack, has a load and a generator connected to it. The demand in the network is assumed to be non-controllable, whereas the generators are assumed to be distributed solar panels with typical PV-type capability constraints given by (13). For this scenario, the capability limits and the values of loads and generation are shown in Table II. In addition to the loads and generation, we consider that a shunt capacitor is connected to bus 2. In order to model this shunt capacitor, we consider that it is part of the first line. In particular, we consider that the shunt capacitance on the sending end of the π-model of the line that connects buses 1 and 2 is modified accordingly, to account for the shunt capacitor. For this particular test case, it is worth noting that ADMM exhibits oscillations and fails to converge to a solution (see Part I, Fig.7-10).

The results for this specific test-case, for the voltage magnitudes and the active and reactive power of the buses, are shown in Fig. 10. It is worth observing that the proposed algorithm converges to a solution within a few tens of iterations; which is contrary to the ADMM-based solution of the OPF problem.

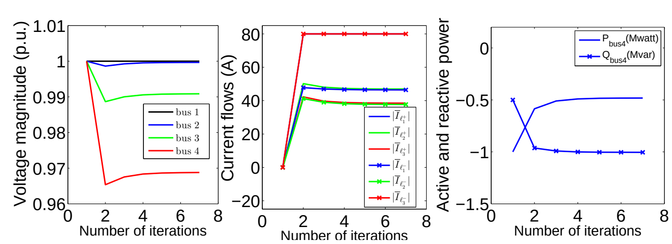

Fig. 9. Evolution of the magnitude of network voltages, current flows, as well as active and reactive power of the controllable load at bus 4 for the case of low generation and high load in the network.

Table II
PARAMETERS OF THE TEST NETWORK USED FOR THE EVALUATION OF ALGORITHM 1 IN THE PRESENCE OF SHUNT CAPACITORS IN THE NETWORK

Parameter	**Value**
Generators' power, $\lvert S_{i_{g_{max}}}\rvert, i = 2,3,4$ (MVA)	$0.40, 0.39, 0.46$
Generators' power factor, $cos\phi_{i_g}, i = 2,3,4$	0.9
Loads' active power, $P_{i_c}, i = 2,3,4$ (MW)	$2.76, 2.16, 2.46$
Loads' reactive power, $Q_{i_c}, i = 2,3,4$ (MW)	$1.38, 1.08, 1.23$
Shunt capacitor (bus 2)(uF)	859
Penalty term gain, ρ	10^4
Tolerance and maximum number of iterations	$10^{-4}, 10^4$
$[V_{min}, V_{max}]$ (p.u)	$[0.9, 1.1]$

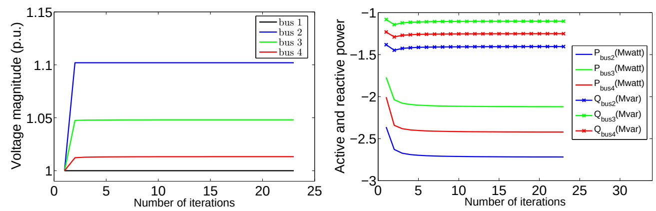

Fig. 10. Evolution of the active and reactive power, as well as the voltages of the buses when a shunt capacitor is connected to bus 2.

C. Performance Evaluation of the Proposed Algorithm under Different Initial Conditions of the Network State

Finally, we investigate the performances of the proposed algorithm under different initial conditions of the network state variables. In order to do so, we initialize the magnitude of the control variables $\bar{E}^0_{\ell+}, \bar{E}^0_{\ell-}, V^0_b$ in Algorithm 1 in the range $[0.9, 1.1]$ and their angle in the range $[-\pi/6, \pi/6]$, totaling 121 different cases. For each combination, we solve the centralized OPF problem for the same network adopted in Part I (Fig. 3). In all the cases the algorithm converges to the same solution within a few tens of iterations. In Table III, the mean value of the number of iterations, as well as the 95-th percentile are shown. For the sake of brevity, we show in Fig. 11-12 the convergence results for the voltage, as well as for the current flows and the active and reactive power profiles for the two extreme cases, specifically when the voltage magnitude is set to 0.9 (1.1) and the voltage angle is set to $-\pi/6$ ($\pi/6$).

Table III
NUMBER OF ITERATIONS FOR THE SOLUTION OF THE OPF PROBLEM (ALGORITHM 1)

	Mean number of iterations	**95-th Percentile**
Algorithm 1	18.21	46.45

IV. PERFORMANCE EVALUATION OF THE PROPOSED DISTRIBUTED ASYNCHRONOUS OPF ALGORITHM

For the sake of completeness, in this section, we assess the performance of the proposed algorithm with respect to a realistic grid represented by a modified IEEE 13-node test feeder ([19]). The modifications are (i) balanced lines, (ii) inclusion of secondary substations where voltage independent PQ-injections are placed, and (iii) lines ten times longer. We

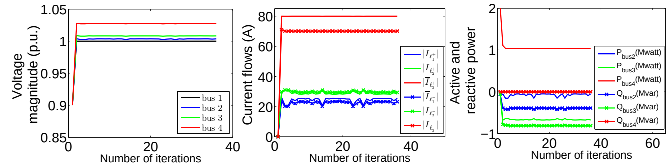

Fig. 11. Evolution of the magnitude of network voltages, line current flows and active and reactive power of the controllable devices when the initial voltage magnitudes are set to 0.9 and the voltage angles to $-\pi/6$.

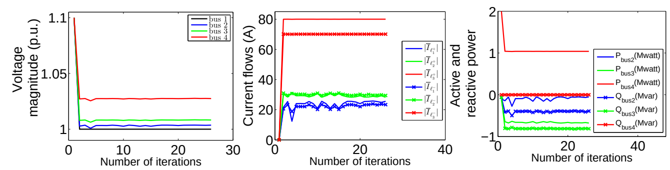

Fig. 12. Evolution of the magnitude of network voltages, line current flows and active and reactive power of the controllable devices when the initial voltage magnitudes are set to 1.1 and the voltage angles to $\pi/6$.

use this benchmark to assess the behavior of the proposed distributed asynchronous OPF algorithm. Also, we compare the solution and convergence of the distributed version of the algorithm to the centralized one.

We consider a test case where each network bus, apart from the slack bus, has a load and a generator connected to it. The demand in the network is assumed to be non-controllable, whereas the generators are assumed to be distributed solar panels with typical PV-type capability constraints. For this test case, the capability limits and the values of loads and generation are shown in Table IV.

We solve the OPF problem in (8)-(13) using Algorithm 1, as well as the asynchronous implementation of Algorithm 2. The results are shown in Fig. 13- 15. For the sake of brevity, we plot only the evolution of the magnitudes of the minimum voltage, the maximum voltage and the median value of the voltage. We plot also the evolution of the minimum, maximum and mean values of the current flows on the receiving-end of the line and the evolution of the active and reactive powers. It is worth observing that Algorithm 1 converges to the optimal solution within a few iterations and also that the distributed asynchronous implementation of Algorithm 1 converges to the same solution as its centralized counterpart.

Table IV
CAPABILITY LIMITS AND VALUES OF LOADS AND GENERATION FOR THE EVALUATION OF ALGORITHM 2

Bus	$S_{g_{max}}$ (MVA)	$P_c(MW)$/ Q_c(Mvar)	**Bus**	$S_{g_{max}}$ (MVA)	P_c(MW)/ Q_c(Mvar)
2	0.0437	0.0025 / 0.0011	8	0.0347	0.0031 / 0.0014
3	0.0480	0.0029 / 0.0012	9	0.0403	0.0031 / 0.0013
4	0.0506	0.0032 / 0.0013	10	0.0373	0.0031 / 0.0013
5	0.0367	0.0029 / 0.0012	11	0.0482	0.0024 / 0.0010
6	0.0443	0.0029 / 0.0012	12	0.0399	0.0030 / 0.0013
7	0.0426	0.0025 / 0.0010	13	0.0436	0.0029 / 0.0012

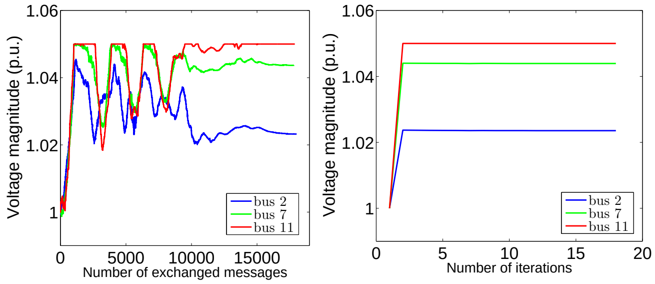

Fig. 13. Evolution of the voltage magnitude for the distributed asynchronous algorithm as a function of the number of messages exchanged (left) and for Algorithm 1 as a function of the number of iterations (right).

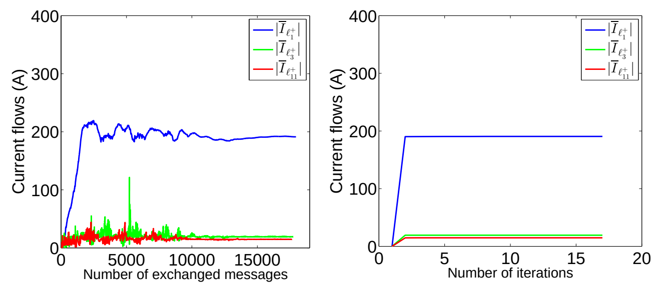

Fig. 14. Evolution of the current flows for the distributed asynchronous algorithm as a function of the number of messages exchanged (left) and for Algorithm 1 as a function of the number of iterations (right).

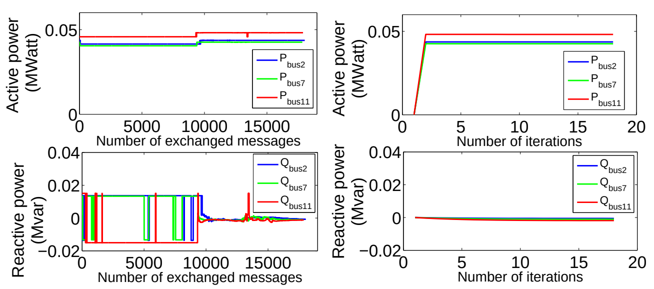

Fig. 15. Evolution of the active and reactive power for the distributed asynchronous algorithm as a function of the number of messages exchanged (left) and for Algorithm 1 as a function of the number of iterations (right).

V. Conclusion

To overcome the limitations identified in Part I, we have proposed algorithms for the solution of the AC non-convex OPF problem in radial networks that are proven to converge to a local minimum. These algorithms use an augmented Lagrangian approach and rely on the method of multipliers for the OPF solution. The two algorithms solve the centralized and decentralized (asynchronous) formulation of the targeted OPF. We have shown the robustness of the centralized version with respect to the following elements: (i) various line lengths, (ii) various network-rated voltage values and (ii) different network operating points (cases where the BFM convexification leads to an incorrect solution), (iii) the presence of shunt capacitors in the grid (where ADMM failed to converge to a solution) and (iv) different initial conditions of the electrical network state. Finally, we have verified the equivalence of the two proposed algorithms for the case of the IEEE 13-node test distribution feeder where realistic operating conditions have been considered.

References

[1] M. Farivar and S. H. Low, “Branch flow model: Relaxations and convexification - part I,” *IEEE Trans. on Power Systems*, vol. 28, no. 3, pp. 2554–2564, 2013.

[2] M. Farivar and S. Low, “Branch flow model: Relaxations and convexification - part II,” *IEEE Trans. on Power Systems*, vol. 28, no. 3, pp. 2565–2572, Aug 2013.

[3] A. X. Sun, D. T. Phan, and S. Ghosh, “Fully decentralized AC optimal power flow algorithms,” in *Power and Energy Society General Meeting (PES)*. IEEE, 2013, pp. 1–5.

[4] T. Erseghe, “Distributed optimal power flow using ADMM,” *IEEE Trans. on Power Systems*, vol. 29, no. 5, pp. 2370–2380, Sept 2014.

[5] D. P. Bertsekas, *Nonlinear Programming*, 2nd ed. Athena Scientific, Sep. 1999.

[6] M. J. Powell, “Algorithms for nonlinear constraints that use lagrangian functions,” *Mathematical programming*, vol. 14, no. 1, pp. 224–248, 1978.

[7] M. R. Hestenes, “Multiplier and gradient methods,” *Journal of optimization theory and applications*, vol. 4, no. 5, pp. 303–320, 1969.

[8] S. Bolognani, R. Carli, G. Cavraro, and S. Zampieri, “A distributed control strategy for optimal reactive power flow with power constraints,” in *52nd Annual Conference on Decision and Control (CDC)*. IEEE, 2013, pp. 4644–4649.

[9] ——, “A distributed control strategy for optimal reactive power flow with power and voltage constraints,” in *IEEE International Conference on Smart Grid Communications (SmartGridComm)*, Oct 2013, pp. 115–120.

[10] E. Dall’Anese, H. Zhu, and G. B. Giannakis, “Distributed optimal power flow for smart microgrids,” *IEEE Trans. on Smart Grid*, vol. 4, no. 3, pp. 1464–1475, 2013.

[11] B. Zhang, A. Lam, A. Dominguez-Garcia, and D. Tse, “An optimal and distributed method for voltage regulation in power distribution systems,” *IEEE Trans. on Power Systems*, vol. PP, no. 99, pp. 1–13, 2014.

[12] M. Kraning, E. Chu, J. Lavaei, and S. Boyd, “Dynamic network energy management via proximal message passing,” *Foundations and Trends in Optimization*, vol. 1, no. 2, pp. 70–122, 2013.

[13] P. Sulc, S. Backhaus, and M. Chertkov, “Optimal distributed control of reactive power via the alternating direction method of multipliers,” *IEEE Trans. on Energy Conversion*, vol. 29, no. 4, pp. 968–977, Dec 2014.

[14] Q. Peng and S. H. Low, “Distributed algorithm for optimal power flow on a radial network,” *arXiv preprint arXiv:1404.0700*, 2014.

[15] D. P. Palomar and M. Chiang, “A tutorial on decomposition methods for network utility maximization,” *IEEE Journal on Selected Areas in Communications*, vol. 24, no. 8, pp. 1439–1451, 2006.

[16] S. Boyd, N. Parikh, E. Chu, B. Peleato, and J. Eckstein, “Distributed optimization and statistical learning via the alternating direction method of multipliers,” *Foundations and Trends® in Machine Learning*, vol. 3, no. 1, pp. 1–122, 2011.

[17] D. Bertsekas, *Constrained Optimization and Lagrange Multiplier Methods*, ser. Athena scientific series in optimization and neural computation. Athena Scientific, 1996. [Online]. Available: http://books.google.ch/books?id=-UQZAQAAIAAJ

[18] A. Geoffrion, “Generalized benders decomposition,” *Journal of Optimization Theory and Applications*, vol. 10, no. 4, pp. 237–260, 1972. [Online]. Available: http://dx.doi.org/10.1007/BF00934810

[19] W. Kersting, “Radial distribution test feeders,” in *Power Engineering Society Winter Meeting, 2001. IEEE*, vol. 2, 2001, pp. 908–912 vol.2.